RESEARCH ARTICLE

Excitotoxic Brain Injury in Adult Zebrafish Stimulates Neurogenesis and Long-Distance Neuronal Integration

Kaia Skaggs,[1] Daniel Goldman,[2,3,4] and Jack M. Parent[1,3,5]

Zebrafish maintain a greater capacity than mammals for central nervous system repair after injury. Understanding differences in regenerative responses between different vertebrate species may shed light on mechanisms to improve repair in humans. Quinolinic acid is an excitotoxin that has been used to induce brain injury in rodents for modeling Huntington's disease and stroke. When injected into the adult rodent striatum, this toxin stimulates subventricular zone neurogenesis and neuroblast migration to injury. However, most new neurons fail to survive and lesion repair is minimal. We used quinolinic acid to lesion the adult zebrafish telencephalon to study reparative processes. We also used conditional transgenic lineage mapping of adult radial glial stem cells to explore survival and integration of neurons generated after injury. Telencephalic lesioning with quinolinic acid, and to a lesser extent vehicle injection, produced cell death, microglial infiltration, increased cell proliferation, and enhanced neurogenesis in the injured hemisphere. Lesion repair was more complete with quinolinic acid injection than after vehicle injection. Fate mapping of *her4*-expressing radial glia showed injury-induced expansion of radial glial stem cells that gave rise to neurons which migrated to injury, survived at least 8 weeks and formed long-distance projections that crossed the anterior commissure and synapsed in the contralateral hemisphere. These findings suggest that quinolinic acid lesioning of the zebrafish brain stimulates adult neural stem cells to produce robust regeneration with long-distance integration of new neurons. This model should prove useful for elucidating reparative mechanisms that can be applied to restorative therapies for mammalian brain injury.

GLIA 2014;62:2061–2079

Key words: radial glia, neural stem cells, brain regeneration, neural repair

Introduction

Neurogenesis persists in the adult mammalian brain in two main regions, the subventricular zone (SVZ) lining the lateral ventricles and the subgranular zone of the dentate gyrus. Neural progenitor cells (NPCs) in the SVZ have been proposed as an endogenous source of new neurons that could be mobilized to repair brain circuits damaged due to injury or disease (Kernie and Parent, 2010). In response to ischemic injury, for example, adult SVZ NPCs proliferate, differentiate, and migrate toward injured areas (Arvidsson et al., 2002; Jin et al., 2001, 2003; Parent et al., 2002; Plane et al., 2004; Yamashita et al., 2006; Zhang et al., 2001). However, most of their neuronal progeny fail to survive or integrate into the preexisting neuronal circuitry, and thus only limited repair occurs following injuries to the mammalian brain (Arvidsson et al., 2002; Parent et al., 2002; Thored et al., 2006). In contrast, extensive areas of constitutive neurogenesis have been described in the brain and other regions of the adult zebrafish central nervous system (CNS) (Adolf et al., 2006; Chapouton et al., 2010; Ganz et al., 2010, 2012; Grandel et al., 2006; März et al., 2010; Zupanc et al., 2005), and zebrafish have the capacity to fully repair injuries to the CNS. For example, robust regeneration persists after injury to the adult fish retina, cerebellum, spinal cord or optic nerve (Becker and Becker, 2007, 2008; Becker et al., 1997; Bernardos et al., 2007; Clint and Zupanc, 2001; Fausett and Goldman, 2006;

View this article online at wileyonlinelibrary.com. DOI: 10.1002/glia.22726

Published online July 15, 2014 in Wiley Online Library (wileyonlinelibrary.com). Received Mar 13, 2014, Accepted for publication July 3, 2014.

Address correspondence to Jack M. Parent, Department of Neurology, University of Michigan Medical School, 5021 BSRB, 109 Zina Pitcher Place, Ann Arbor, Michigan 4810-2200, USA. E-mail: parent@umich.edu

From the [1]Departments of Neurology, University of Michigan Medical Center, Ann Arbor, Michigan; [2]Biological Chemistry, University of Michigan Medical Center, Ann Arbor, Michigan; [3]Neuroscience Graduate Program, University of Michigan Medical Center, Ann Arbor, Michigan; [4]Molecular and Behavioral Neuroscience Institute, University of Michigan Medical Center, Ann Arbor, Michigan; [5]VA Ann Arbor Healthcare System, Ann Arbor, Michigan.

Additional Supporting Information may be found in the online version of this article.

Hui et al., 2010; Reimer et al., 2008; Sirbulescu and Zupanc, 2011; Veldman et al., 2007, 2010; Yurco and Cameron, 2005; Zupanc, 2008; Zupanc and Ott, 1999; Zupanc and Zupanc, 2006). Several recent studies have also demonstrated that zebrafish can repair physical damage to the telencephalon following stab injuries, and that this repair involves stimulation of neurogenesis from radial glial progenitors (Ayari et al., 2010; Diotel et al., 2013; Kishimoto et al., 2012; Kizil et al., 2012a, 2012b; Kroehne et al., 2011; Kyritsis et al., 2012).

Radial glial NPCs line the everted ventricular surface and medial lumen of the adult zebrafish brain. These ventricular zone (VZ) cells exhibit characteristics similar to those of mammalian neural stem cells, such as expression of glial fibrillary acidic protein (GFAP), relative quiescence, differentiation into amplifying progenitors and generation of neurons throughout life. In the uninjured brain, most NPCs divide slowly with characteristics of both symmetric self-renewing and asymmetric neurogenic divisions (Ganz et al., 2010; März et al., 2010; Pellegrini et al., 2007; Rothenaigner et al., 2011). Lineage tracing in the intact zebrafish brain shows that new neurons migrate a short distance from the VZ and integrate into neural circuitry as indicated by the presence of synaptic vesicles and firing of action potentials (Rothenaigner et al., 2011). The persistence of neural stem cells and robust neurogenesis in the adult offers a fertile substrate for tissue repair after injury.

We sought to exploit the robust regenerative capacity of the adult zebrafish CNS to establish a novel brain injury model to study the restorative properties of adult zebrafish brain in a disease-relevant context. To this end, we employed a zebrafish brain lesioning model using forebrain injection of the excitotoxin quinolinic acid (QA). QA is a well-characterized neurotoxic metabolite of the kynurenine pathway that acts as an agonist at *N*-methyl-D-aspartate (NMDA) receptors. Susceptibility to QA-induced excitoxicity varies by brain region, with forebrain neurons in the neocortex, striatum, and hippocampus being particularly sensitive (Guillemin, 2012; Schwarcz and Köhler, 1983). Initial interest in QA was stimulated by observations of its convulsant effects (Lapin, 1978) and ability to cause selective striatal neuron loss with pathology similar to Huntington's disease (HD) (Beal et al., 1986; Ferrante et al., 1993; Schwarcz and Köhler, 1983). In addition to studies of rodent striatal lesioning with QA as an HD model, several groups have employed QA injections into rodent brain to model cerebral ischemic insults (Darlington et al., 2007; Schwarcz et al., 2012; Stone et al., 2012; Zwilling et al., 2011). When injected into the striatum of adult rodents to model HD, QA lesioning strongly stimulates SVZ and striatal neurogenesis (Collin et al., 2005; Tattersfield et al., 2004). However, the extent of repair is very limited in these models.

Given the widespread use of QA-induced brain injury in rodents to model human neurological disorders, we sought to examine QA lesioning of adult zebrafish telencephalon to determine whether a robust neurogenic response leads to more complete brain repair. We found that QA-induced telencephalic injury in adult zebrafish potently stimulates neural stem cell proliferation, migration and integration of new neurons to repair the injury in a more robust and extensive manner than injuries caused by vehicle alone. Given the pathophysiological relevance of QA-induced brain injury models of HD and stroke, these results provide a powerful new tool for investigating neuronal regeneration in a vertebrate system. This fish model should prove useful for studying the biological basis of regeneration as well as for testing potential therapies that might enhance the regenerative response in the mammalian brain.

Materials and Methods

Animal Care

Fish were kept under standard conditions at 26–28°C on a 14-h light/10-h dark cycle and were observed daily for health. All animal care and experimental procedures were carried out in accordance with guidelines and approval of the University Committee on Use and Care of Animals at the University of Michigan. All fish were obtained from in-house breeding colonies. The following transgenic fish lines were previously described: Tg(*1016tuba1a:GFP*) (Fausett and Goldman, 2006), Tg(*her4.1:CreER^{T2}*) (Boniface et al., 2009), Tg(*β-actin2:loxP-mCherry-loxP-GFP*) (Ramachandran et al., 2010), Tg(*gfap:GFP*) (provided by David Hyde, University of Notre Dame, (Ramachandran et al., 2011)), Tg(*ascl1a:GFP*) (Wan et al., 2012), and Tg(*olig2:GFP*) (provided by Bruce Appel, University of Colorado, (Shin et al., 2003)). Double transgenic Tg(*her4.1:CreER^{T2};β-actin2:loxP-mCherry-loxP-GFP*) fish were generated through in-house breeding.

QA Lesioning

Adult fish (6–24 months old) were anesthetized in 0.02% ethyl 3-aminobenzoate methanesulfonate (Tricaine, Fluka) until unresponsive to tail pinch. Fish were placed in a clay mold under a dissecting stereomicroscope. A Hamilton syringe with a 30-gauge needle cut to a length of approximately 3 mm was loaded with 2.5 μL of 15 mM 2,3-Pyridinedicarboxylic acid (quinolinic acid, QA, Aldrich) in 0.99% sterile saline or with saline alone. The needle was inserted vertically through the intact skull into the right telencephalic hemisphere using eye position and visible skull sutures as guides and QA or vehicle was injected. Fish were returned to clean fish water and observed for recovery. Fish unable to swim or feed following injury (<5%) were euthanized immediately with an overdose of Tricaine. In double transgenic Tg(*her4.1:CreER^{T2};β-actin2:loxP-mCherry-loxP-GFP*) fish, recombination was induced through intracranial injection of tamoxifen (1.25 μL of a 50 μM solution) dissolved in 100% ethanol in combination with QA (1.25 μL of a 30 mM QA solution for a final concentration of 15 mM in 2.5 μL) or vehicle (1.25 μL for a total volume of 2.5 μL).

Some uninjured control fish received intraperitoneal (i.p.) tamoxifen (10 μL of a 50 μM solution) daily for 4 days.

Cell Proliferation and Cell Death Assays

Adult fish (6 months – 2 years old) were anesthetized in 0.02% Tricaine and injected intraperitoneally with 10μL of 10 mg/ml bromodeoxyuridine (BrdU) or 10 μL of 10 mg/ml 5-ethynyl-2′-deoxyuridine (EdU) as indicated. EdU was detected using the manufacturer's protocol for ClickIt EdU Imaging (Invitrogen). To assay for cell death, the terminal deoxynucleotidyl transferase deoxyuridine triphosphate nick-end labeling (TUNEL) stain was performed with the ApopTag peroxidase direct *in situ* detection kit (Millipore) using the manufacturer's protocol.

Tissue Preparation

Fish were anesthetized in 0.02% Tricaine until unresponsive to tail pinch and intracardially perfused with phosphate-buffered saline (PBS) followed by 4% paraformaldehyde (PFA) for 3 min. Brains were dissected from the skull and incubated in 4% PFA at room temperature for 3 h, washed in PBS, and cryoprotected in 20% sucrose overnight at 4°C. Brains were embedded in tissue freezing medium (TFM, Triangle Biomedical Sciences) and stored at −80°C until sectioning. Frozen sections were cut using a cryostat (Leica CM1850) at 12 μm thickness and directly mounted onto coated glass slides.

Histology and Microscopy

Hematoxylin and eosin (H&E) staining were performed using standard protocols. Briefly, slides with frozen sections were left to thaw and dry at room temperature for 30 min. They were post-fixed in 4% PFA for 20 min, followed by two washes in PBS (5 min) and water (2 min). Slides were immersed for 2 s in hematoxylin (Sigma) and rinsed by agitation in tap water for 1 min. Slides were then dipped in eosin (Fisher), dehydrated (30 sec each in 95%, 95%, 100%, and 100% EtOH), cleared in Xylene, and mounted with Permount (Fisher).

To perform immunofluorescence histochemistry, slides with frozen sections were left to thaw and dry at room temperature for 20 min, followed by 5-min rinses × 3 in TBS and incubation for 1 h at room temperature in blocking buffer (TBS, 0.4% Triton X-100, 3% normal goat serum). Primary antibodies were diluted in blocking buffer with overnight incubation at 4°C. Primary antibodies were detected using Alexa-488- or Alexa-594-conjugated secondary antibodies raised in goat against the appropriate primary antibody species (1:300, Invitrogen) by incubation at room temperature for 90 min. This was followed by a 15-min incubation with bisbenzimide to counterstain cell nuclei. Following additional rinses with TBS, slides were coverslipped using Prolong AntiFade (Invitrogen) mounting reagent. Primary antibodies used were: mouse anti-4C4 (1:250, kind gift of Pamela Raymond), sheep anti-BrdU (1:100, Abcam), rabbit anti-calretinin (1:500, Swant), rabbit anti-GABA (Sigma, 1:500), rabbit anti-GFAP (1:250, Dako), rabbit anti-GFP (1:1000, Molecular Probes), chick anti-GFP (1:1000, Aves), mouse anti-HuC/D (1:250, Molecular Probes), mouse anti-SV2 (1:1000, Developmental Studies Hybridoma Bank), and mouse anti-tyrosine hydroxylase (1:250, ImmunoStar). Images were obtained using a Leica DMI 6000B epifluorescence microscope equipped with a Hamamatsu digital camera, a Leica DM-IRB microscope equipped with a Spot Flex digital camera system, or a Leica MP inverted confocal microscope. Brightness and contrast were adjusted uniformly for whole images when needed using Adobe Photoshop CS5.1, and composite panels were assembled using Adobe Illustrator CS5.1.

Cell Counting and Statistical Analysis

Area of microglial immunoreactivity was calculated using ImageJ software on individual 12 μm sections located approximately 60 μm apart within each brain from at least three sections per brain and four brains per condition. Manual threshold adjustment was verified by masking outlines on each section before counting. Proliferative cells were counted on individual 12 μm sections located approximately 60 μm apart within each brain from at least three sections per brain and four brains per condition and summed using ImageJ software. Two independent counts of 10 (out of 100) sections established a reliability of 98%. TUNEL-positive cells were counted on individual 12 μm sections located approximately 60 μm apart ($n = 9$ per condition) and summed using ImageJ software. All statistical analyses were conducted using SPSS Version 20 or 22.

Results

QA Lesion Model

To determine whether QA injection produces focal lesions in the adult zebrafish brain, we injected a range of QA concentrations (1–15 mM) and volumes (1–2.5 μL) into the right telencephalic hemisphere of adult zebrafish. Externally visible skull sutures and eye position were used to guide the injection site. We found that injection of 2.5 μL of a 15 mM QA solution produced the most consistent injury (Fig. 1A and data not shown). This QA dose or an equivalent volume of saline was used for all subsequent experiments. The contralateral hemisphere served as an internal control for each condition and the vehicle injection served as a non-excitotoxic injury control. Fish injected with QA showed a characteristic behavioral response to the excitotoxic lesion that vehicle-injected controls did not exhibit. Upon recovering from anesthesia, QA-lesioned fish circled in an ipsilesional (clockwise) direction and occasionally exhibited corkscrew swimming (see Supp. Info. Movie). This behavior is similar to the circling seen in rodents after QA-induced striatal injury (Schwarcz et al., 1979; Ungerstedt, 1971), lasted 1–2 h after QA injection, and was not seen after vehicle injection of the fish.

We next examined the extent of telencephalic damage by TUNEL staining to label apoptotic cells. Within 4 h after QA or vehicle injection, many TUNEL-positive cells appeared near the injury site with rare labeled cells in the contralesional hemisphere (Fig. 1C–E). TUNEL staining increased further by 1 day following injury (Fig. 1F–H), with more labeled cells after lesioning with QA than vehicle in the injured hemisphere (Fig. 1B). TUNEL staining remained

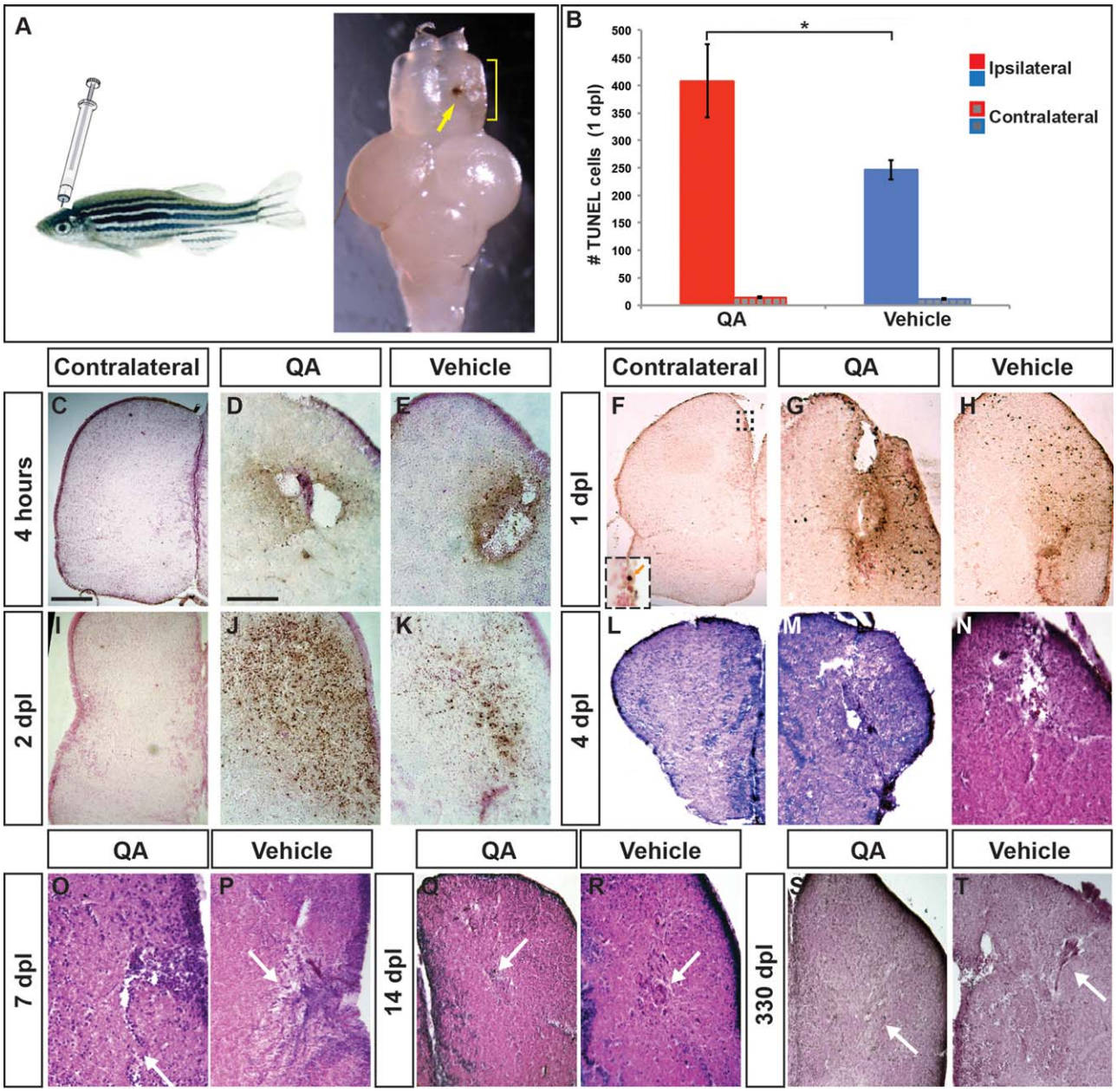

FIGURE 1: Telencephalic injury with QA results in early cell death followed by repair. (**A**) The adult zebrafish telencephalon was lesioned by injecting QA or vehicle orthogonally into the right hemisphere to a depth of approximately 2 mm. Two days postinjury, a blood clot identifies the injection track (arrow) and tissue disruption can be seen in the damaged hemisphere (yellow bracket). (**B–K**) Cell death was examined using a TUNEL assay. (B) The number of TUNEL-positive cells was quantified in the injured and uninjured hemispheres 1 day following QA or vehicle injection. Results from a one-way analysis of variance (ANOVA) indicated that both types of injury increased cell death, with more TUNEL-positive cells in the injured hemisphere following QA- than vehicle-induced injury ($F(1,16) = 4.928$, $P < .05$, $n = 9$). There was no difference in the number of TUNEL-positive cells on the contralateral side between QA and vehicle injuries ($F(1,16) = 1.755$, n.s.). (C, F, I) Very few apoptotic cells were seen on the uninjured side of the telencephalon following QA lesions (inset in F). (D,E) Dying cells appear near the injury site within 4 h after injury both in QA (D) and vehicle (E) conditions. (G,H) At 24 h postinjury the area of TUNEL reactivity has expanded in both QA- (G) and vehicle-injected (H) fish. TUNEL positive cells can be seen some distance from the injection site. (J,K) TUNEL positive cell numbers peak at 48 h postinjury, with a more extensive area of TUNEL reactivity in QA- (J) than vehicle-injured (K) brains. (**L–T**) H & E staining reveals extensive damage 4 days following both QA (M) and vehicle (N) lesions as shown by tissue loss at the site of injury and spongiform appearance in the surrounding areas. By 7 days post-lesion, tissue healing is apparent (white arrows in O, P), particularly following QA-induced lesions, and extensive repair is evident in lesioned tissue at 14 days post-lesion (white arrows in Q, R). More residual fibrous tissue was often seen following vehicle-induced lesions compared with QA-lesioned tissue. At 330 days post-lesion, morphological structure is largely intact in both QA- (S) and vehicle-lesioned (T) brains. Similar to early timepoints, fibrous remnants of vehicle-induced lesions are typically evident (arrow in T). Scale bar = 100 μm. Scale bar in C applies to F, I, L, M, S; scale bar in D applies to E, G, H, J, K, N, O, P, Q, R, T. [Color figure can be viewed in the online issue, which is available at wileyonlinelibrary.com.]

high at 2 days post lesion (dpl; Fig. 1I–K) with apoptosis declining over the subsequent days (data not shown). Interestingly, TUNEL$^+$ cells were not only detected in a wide area surrounding the lesion site, but also appeared in the VZ distant from the lesion and in the contralateral VZ (Fig. 1F inset and data not shown).

Tissue damage resulting from the QA or vehicle injection was next examined using H&E staining. At 4 dpl, extensive telencephalic damage was evident both at the injury site and extending into the surrounding parenchyma (Fig. 1L–N). Tissue disruption and spongioform changes were similar in QA- (Fig. 1M) and vehicle-induced (Fig. 1N) lesions. The contralesional hemisphere was unaffected by QA or vehicle injection (Fig. 1L and data not shown). As expected, immunostaining for the neuronal marker HuC showed a loss of neurons in the injured region (data not shown).

By 7 dpl, hematoxylin-stained cells were evident in large numbers near the lesion site and the spongioform appearance of the surrounding tissue was considerably reduced, particularly in QA-lesioned brains (Fig. 1O,P). In many vehicle-injured brains, there was evidence of tissue repair but also the appearance of fibrous structures not observed following QA-induced lesions (Fig. 1O,P, arrows). Similarly, by 2 weeks after injury, the overall tissue morphology appeared relatively restored in the QA-lesioned hemisphere (Fig. 1Q), suggesting nearly complete repair, whereas often the vehicle-lesioned hemisphere retained evidence of injury in the form of a scar-like structure (Fig. 1R). By this time point following injury, the distribution of HuC/D-expressing neurons in the injured telencephalic hemispheres appeared largely the same as the noninjured hemisphere (data not shown). In the chronic stage, between 2 and 11 months after QA injection, the lesion site was undetectable except at the dorsal-most aspect of some brains (Fig. 1S). As at earlier timepoints, vehicle-induced lesion sites often retained a small area of accumulated cell debris and morphological changes as late as 11 months following injury, also more prominently in the dorsal aspects of the injured hemisphere (Fig. 1T). These results demonstrated that QA-induced lesioning is a viable injury model in adult zebrafish, and that repair is more complete following QA lesions than vehicle lesions despite initially greater cell death. These findings led us to ask what processes might be responsible for the differences in healing.

Microglial Response to QA Lesioning

One of the hallmarks of the mammalian response to brain injury is reactive gliosis (Robel et al., 2011; Sofroniew, 2005). The initial glial response is comprised of microglial and astrocytic elements that are thought to exert both positive and negative influences on the eventual degree of damage; however, later astroglial scarring is considered a major barrier to regeneration in mammals, adversely affecting axonal outgrowth and neuronal survival (reviewed in Fitch and Silver, 2008; Robel et al., 2011; Sofroniew, 2005; Yiu and He, 2006). We first assayed for a microglial reaction to QA lesioning of the zebrafish telencephalon. We found a massive microglial response that began within the first 24 h after injury (Fig. 2A–D). Large areas of the injured hemisphere contained many overlapping microglia as shown by immunostaining with the zebrafish microglial marker 4C4 (Becker and Becker, 2001), reaching a maximum at about 2 days post injury (Fig. 2E–H,Y). Increased numbers of microglia were also seen in the contralesional hemisphere, but to a far lesser extent than ipsilesionally. In addition, many of the 4C4-labeled cells exhibited the appearance of activated microglia, with rounded, highly branched morphology typical of active phagocytes. Microglial numbers remained high throughout the injured hemisphere for 7–10 dpl (Fig. 2I–P,Y) and then gradually declined (Fig. 2Q–T,Y). However, increased numbers of microglia persisted at the injury site for at least several weeks. Double labeling with the mitotic marker EdU, which was administered as a single pulse on day 1 after QA (2 h before perfusion), showed that some of the microglia in the injured hemisphere were proliferative (Fig. 2U–U‴). At all timepoints observed, microglial activation was more widespread following QA-induced injury relative to vehicle injections in both the ipsilesional and contralesional hemispheres (Fig. 2Y).

In the mammalian brain, Olig2-expressing glial cells respond to injury with increased proliferation and contribute to the formation of a glial scar (Buffo et al., 2005; Sofroniew, 2009). We therefore examined the oligodendrocyte lineage response to QA- and vehicle induced injury using Tg(*olig2:GFP*) fish to label oligodendrocyte lineage cells (Shin et al., 2003). In the uninjured hemisphere, GFP-expressing oligodendroglia were dispersed throughout the parenchyma (Supp. Info. Fig. 1A,D). By 2 days following vehicle-induced injury, GFP-expressing cells began to accumulate near the lesion site (Supp. Info. Fig. 1C) and slightly more persisted at 7 dpl (Supp. Info. Fig. 1F), likely due to oligodendrocyte progenitor proliferation (Supp. Info. Fig. 1C′,F′, arrows), consistent with previously published results (Baumgart et al., 2011; März et al., 2011). In contrast, QA lesions resulted in a loss of GFP-expressing cells near the lesion site and severe morphological changes in the remaining GFP-labeled oligodendrocytes at 2 dpl (Supp. Info. Fig. 1B), consistent with the observation that oligodendrocytes are vulnerable to QA-induced excitotoxicity (Benjamins et al., 2013; Cammer, 2001; Karadottir et al., 2005). By 7 days following QA induced lesions, GFP-expressing oligodendrocytes accumulated near the QA lesion site (Supp. Info. Fig. 1E). The increased numbers probably reflect a combination of

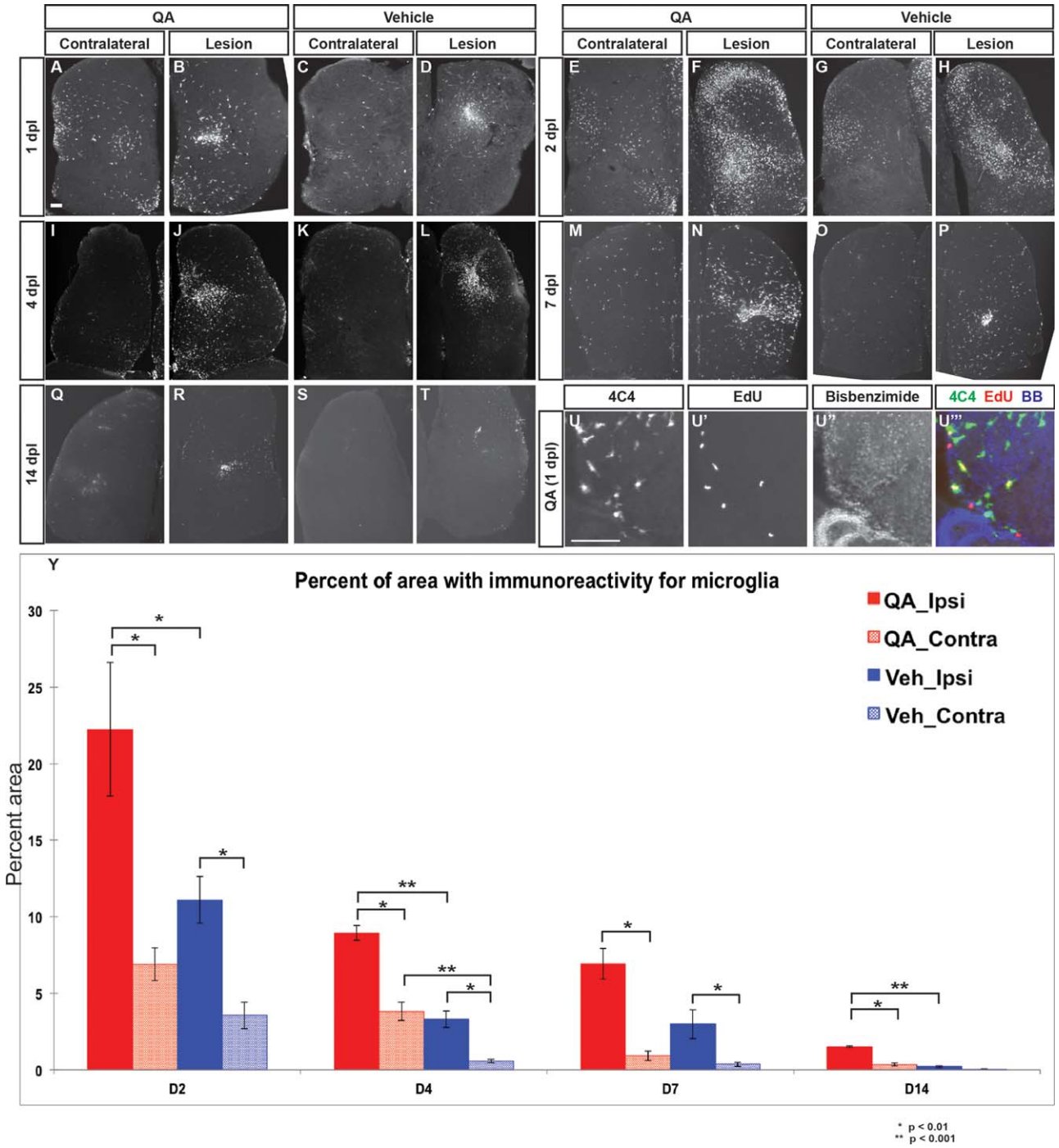

FIGURE 2: Microglial response to telencephalic injury is rapid and extensive. (**A,D**) Within 24 h post injury, 4C4-immunoreactive microglia appear in large numbers in the ipsilesional telencephalic hemisphere following both QA- (**B**) and vehicle-induced (D) lesions. Substantial numbers of microglia are also seen in the contralesional hemisphere (A, **C**) compared with the intact brain. (**E–H**) Microglial numbers peak at 48 h post injury in both the ipsilesional (F,H) and contralesional (E,G) hemispheres, with more widespread microglial presence in QA- (E-F, **Y**) relative to vehicle-induced (G,H,Y) injury. (**I–T**) The microglial response persists at lower levels on days 4 and 7 after injury, and returns toward baseline levels by 14 days. (**U–U‴**) Microglia in the parenchyma proliferate as an early response to injury as shown by incorporation of EdU 24 h post-lesion. (Y) Quantification of the microglial reaction after QA or vehicle lesioning. The percent area of 4C4 immunoreactivity is more extensive following QA-induced than vehicle-induced injury in the ipsilesional hemisphere at all timepoints measured as well as in the contralesional hemispheres at 2, 4, and 14 dpl. ANOVA results indicated significant main effects for lesion type ($F(1, 66) = 24.586$, $P < 0.0001$), dpl ($F(3, 66) = 37.330$, $P < 0.0001$), and hemisphere ($F(1, 66) = 46.988$, $P < 0.0001$), with significant interaction effects for type of lesion x dpl ($F(3, 66) = 3.577$, $P < 0.018$), type of lesion x hemisphere ($F(1, 66) = 6.051$, $P < 0.017$), and dpl x hemisphere ($F(3, 66) = 9.491$, $P < 0.0001$). Significant post hoc analyses (Tukey HSD) were followed by pairwise comparisons with Bonferroni correction; significant results are indicated on the graph. Scale bar = 100 μm. [Color figure can be viewed in the online issue, which is available at wileyonlinelibrary.com.]

migration and proliferation, with limited incorporation of EdU into GFP+ cells at 2 dpl that increased by 7 dpl (Supp. Info. Fig. 1B′,E′, arrows).

NPC Activation and Proliferation After Injury

NPCs proliferate and give rise to neurons in the adult zebrafish throughout the CNS VZs (Adolf et al., 2006; Chapouton et al., 2010; Ganz et al., 2010, 2012; Grandel et al., 2006; März et al., 2010; Zupanc et al., 2005). This persistent neurogenic capacity is hypothesized to contribute to the robust regenerative response in adult zebrafish following CNS injury. We therefore investigated proliferation following QA- or vehicle-induced lesioning by pulse labeling with the mitotic markers EdU or BrdU 2 h before perfusing fish at various survival times after injury. Proliferation began to increase within 24 h post injury in both the parenchyma and VZ proliferative regions (Fig. 3A–D). Proliferation peaked 2 days after injury with large numbers of EdU^+ or $BrdU^+$ cells in the VZs and parenchyma of the damaged hemisphere (Fig. 3E–H,M), was still considerably elevated at 4–7 days (Fig. 3I–L,M), and remained slightly above control levels at 14 days following lesioning (Fig. 3M). QA-induced injury also substantially increased proliferation in the contralesional hemisphere (Fig. 3E), whereas the increase in proliferation in the uninjured hemisphere was less pronounced after vehicle injection (Fig. 3G). In fact, QA-induced lesions stimulated proliferation in the contralesional hemisphere as robustly as that seen in the damaged hemisphere following vehicle injection for the first 4 days after injury (Fig. 3M). The time course and pattern of QA- or vehicle-induced proliferation were similar on the ipsilesional side of the brain, with more extensive proliferation following QA- relative to vehicle-induced injury at all timepoints examined (Fig. 3M; Supp. Info. Table 1). These results suggest that excitotoxic injury with QA produces a more robust and widespread proliferative response than a stab wound alone (vehicle injection).

We next examined the identity of progenitor cells in the VZs of the zebrafish telencephalon that respond to QA-induced injury using transgenic fish carrying NPC-specific reporters. NPCs in the VZ express radial glial markers such as glial fibrillary acidic protein (GFAP), brain lipid binding protein (BLBP), and S100β (Adolf et al., 2006; Grandel et al., 2006; März et al., 2010). We first examined GFP expression using a Tg(*gfap:GFP*) transgenic reporter fish line to identify radial-glial like neural stem cells. Four days following QA-induced telencephalic lesioning, upregulation of GFP expression was seen in the injured hemisphere, well above the constitutive level of expression found in the contralesional hemisphere (Fig. 4A). We observed increased GFP expression in the VZ on the injured side as well as hypertrophic $GFAP^+$ processes extending into the parenchyma (Fig. 4B–B″). Many of the presumptive neural progenitors expressing GFP in the VZ were proliferating in response to injury (Fig. 4D,E). Those cells that incorporated the mitotic marker EdU and remained in the VZ continued to express GFP, whereas mitotic cells that migrated away from the VZ did not express GFP, indicating that they were no longer radial glia. Processes of GFP-expressing cells extended from the VZ to the area of injury, providing a potential scaffolding for the migration of putative newborn neurons toward the injury site (Fig. 4C,F).

We further examined progenitor response to lesioning using an injury-responsive transgenic reporter line of zebrafish, Tg(*1016tuba1a:GFP*), in which a 1016-base pair fragment of the neural-specific α1 tubulin promoter (*tuba1a*) drives green fluorescent protein (GFP) expression in NPCs of the developing and regenerating adult CNS, but not in regenerating axons of mature neurons (Fausett and Goldman, 2006; Ramachandran et al., 2010). In the intact telencephalon of adult Tg(*1016tuba1a:GFP*) zebrafish, GFP was sparsely expressed in the VZ and completely absent from the parenchyma (Fig. 4G). Four days after QA-induced lesioning of the fish, GFP expression increased markedly in the injured hemisphere (Fig. 4I). GFP^+ processes extended from the VZ toward the lesion site within the injured hemisphere. The GFP-labeled cells proliferated in response to injury as seen by incorporation of EdU given 2 days post injury at the peak of proliferation (Fig. 4I′–J). In contrast, GFP expression was only slightly increased in the VZ of the contralesional hemisphere, mainly in proliferating progenitors (Fig. 4H). Vehicle-induced lesions produced similar results albeit with more restriced expression of the GFP reporter (Supp. Info. Fig. 2A–B″). These findings indicate that normally quiescent progenitors are activated to proliferate following excitotoxic injury.

The proneural gene *ascl1a* has a highly conserved role in promoting neuronal fate specification during development and in adult neurogenic zones (Bertrand et al., 2002; Kim et al., 2011). *Ascl1*-lineage cells contribute to ischemia-induced neurogenesis in adult rodents (Zhang et al., 2011), and are essential for neuronal regeneration in zebrafish following retinal injury (Fausett et al., 2008). We used a *Tg(ascl1a:GFP)* zebrafish line (Wan et al., 2012) to examine the response of ascl1a-expressing cells to telencephalic injury. As expected, in the intact brain and uninjured hemisphere of lesioned brains, modest GFP expression was seen in scattered cells in periventricular regions (Fig. 4K,L). In the QA-lesioned hemisphere, however, GFP expression increased markedly within 4 days after injury (Fig. 4M). GFP^+ cells appeared to extend from the VZ toward the lesion site, and most coexpressed the neuronal marker HuC/D by four dpl (Fig. 4M–N). Many of the GFP-expressing VZ cells proliferated in response to injury (data not shown). GFP expression

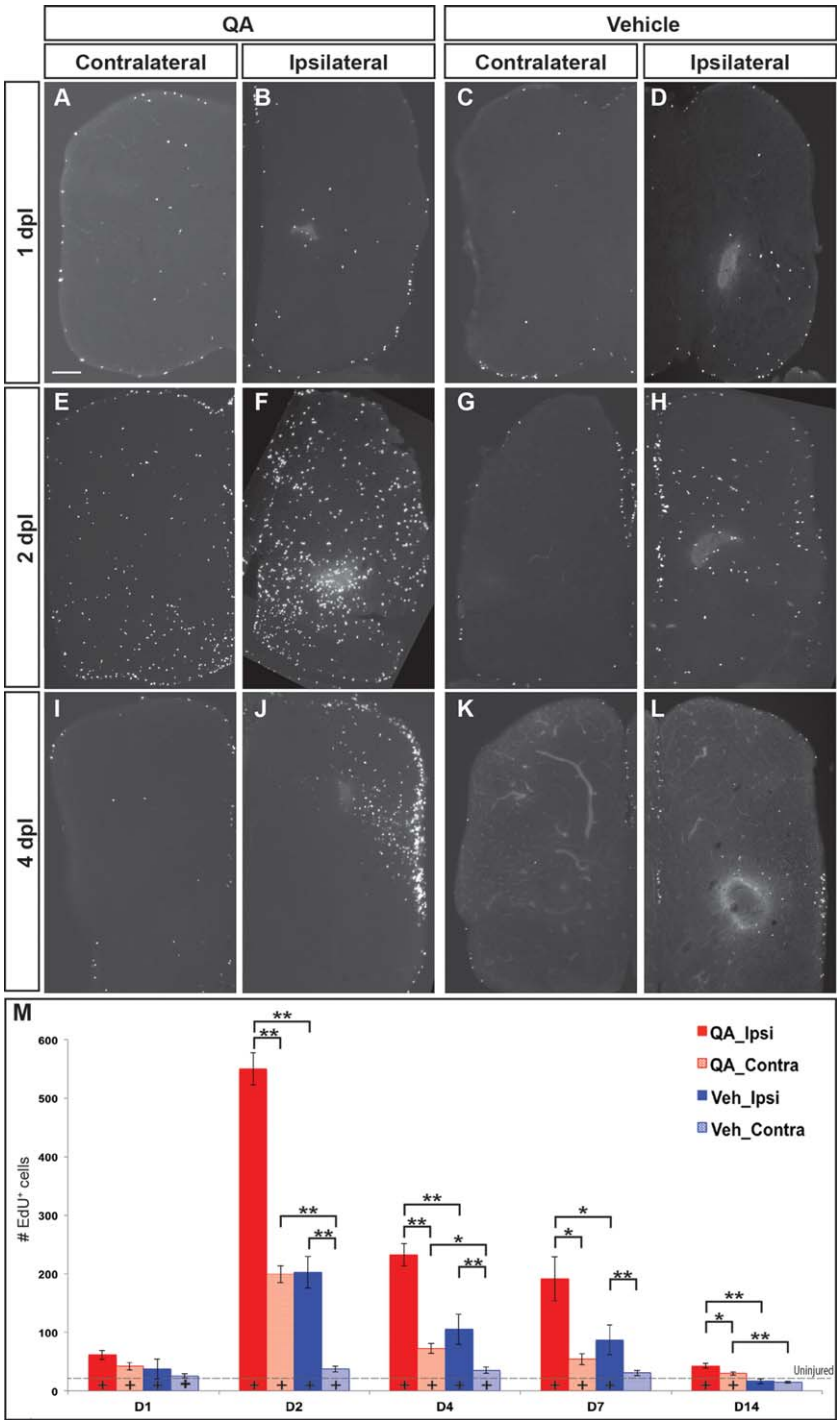

FIGURE 3: Cell proliferation increases dramatically following injury. (**A–D, M**) At 1 day post injury, proliferation began to increase in the VZs and parenchyma of the lesioned telencephalic hemispheres. (**E–H,M**) Extensive proliferation was evident in both ipsilesional and contralesional hemispheres by 2 dpl, especially in the germinative zones and throughout the parenchyma of the ipsilesional hemispheres after QA- more than vehicle-induced lesions. (**I–L,M**) The number of proliferative cells was elevated to a lesser extent at 4 (I–L) and 7 (M) dpl and remained only slightly increased at 14 days (M). (M) Proliferating cell numbers were quantified at various timepoints following QA- (red) or vehicle-induced (blue) injury in the ipsilesional (solid) and contralesional (hatched) telencephalic hemispheres. ANOVA results indicated significant main effects on proliferation for lesion type ($F(2, 76) = 81.943$, $P < 0.0001$) and dpl ($F(8, 154) = 21.224$, $P < 0.0001$), as well as a significant interaction effect for type of lesion x dpl ($F(8, 154) = 14.482$, $P < 0.0001$). Post hoc analyses (Tukey HSD) for proliferation across type of lesion indicated significant differences in proliferation in the injured hemisphere among QA-lesioned, vehicle-lesioned and uninjured brains, and in the uninjured hemisphere between QA-lesioned and vehicle-lesioned or uninjured brains. Results from pairwise comparisons within each day (Student's *t*-test with additional Bonferroni corrections) and with uninjured telencephalic hemispheres are indicated on the graph and in Supporting Information Table 1. *, $P < 0.01$; **, $P < 0.001$; $^{+}$, $P < 0.01$ compared with uninjured (denoted by the dashed horizontal line). Scale bar = 100 μm. [Color figure can be viewed in the online issue, which is available at wileyonlinelibrary.com.]

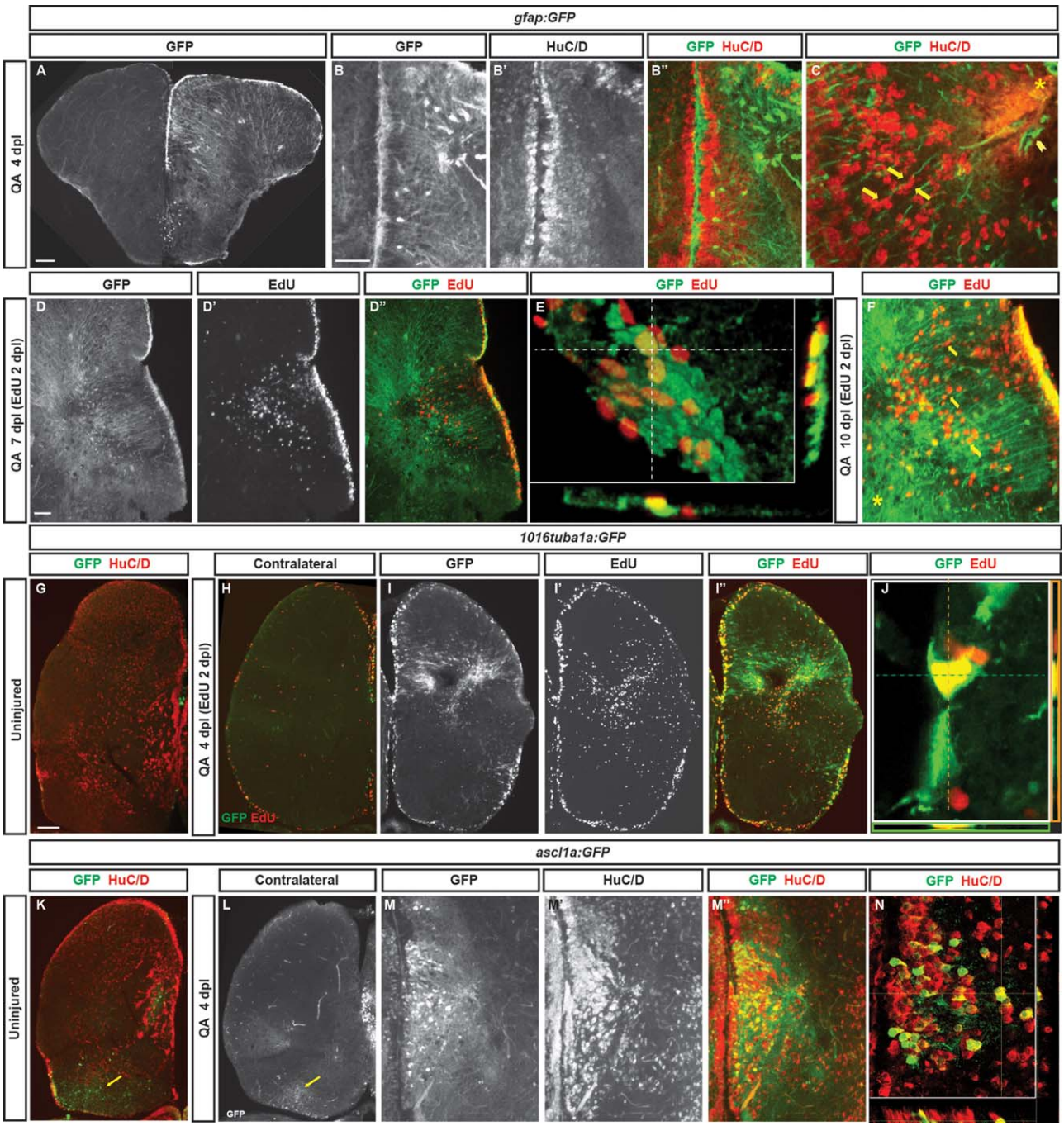

FIGURE 4: Radial glial-like progenitors respond to injury by proliferation and generation of new neurons. (**A**) Coronal section of the telencephalon of a QA-lesioned Tg(*gfap:GFP*) zebrafish shows activation of *gfap* manifest by GFP labeling in radial glial-like progenitors throughout the neurogenic regions in the injured hemisphere (right side of panel) in contrast to the low level of constitutive activity in the uninjured hemisphere at 4 dpl. (**B–B″**) Expanded GFP expression (green) is seen in radial glial-like progenitors located in the VZ as well as hypertrophic GFP-expressing processes within the parenchyma in response to QA-induced lesion. HuC/D in red. (**C**) Double immunostaining for GFP (green) and HuC/D (red) in QA-lesioned brains at 4 dpl shows clusters of HuC/D$^+$ neurons in close proximity to GFP$^+$ processes that extend from the medial VZ to the injury (arrows indicate examples). These processes terminate in structures resembling endfeet near the lesion location (arrowhead). (**D–D‴**) By 7 dpl, horizontal sections show that proliferative GFP$^+$ (green) radial glial-like progenitors that incorporated EdU (red) 5 days earlier persist in the VZ, while EdU-labeled cells that appear to have migrated from the VZ to the injury site no longer express GFP (inset magnified in D‴). (**E**) Orthogonal projection shows colocalization of GFP and EdU at 7 dpl. (**F**) At 10 dpl, costaining for EdU and GFP indicates that many of the newborn cells have migrated substantial distances toward the injury site from the lateral VZ, appearing in close proximity to or in contact with GFP$^+$ processes (arrows indicate examples). (**G–J**) Tg(*tuba1a:GFP*) zebrafish show minimal GFP expression (green) in the uninjured telencephalon (G), increased expression mainly in the VZ of the contralesional hemisphere at 4 dpl (H), and massively increased GFP labeling in the lesioned hemisphere (I–I″) in both the VZ and parenchyma at the injury site. Many GFP$^+$ cells were proliferating 2 days earlier (at 2 dpl) as indicated by EdU incorporation (I″, J). (**K–N**) Tg(*ascl1a:GFP*) fish show a low level of VZ, periventricular and caudal (yellow arrows) GFP labeling (green) in the uninjured state (K) or contralateral to QA injection at 4 dpl (L). In the injured hemisphere, GFP expression increases markedly at 4 dpl in the VZ and periventricular region, and many of the cells coexpress HuC/D (M–N; red in K, M″, and N). Scale bar = 100 μm.

was also found in a population of cells showing a mature neuronal morphology in the caudal telencephalon of both intact and injured fish (arrows in Fig. 4K,L). Vehicle-induced lesions produced similar results in both Tg(*1016tuba1a:GFP*) and Tg(*ascl1a:GFP*) lines, although GFP expression appeared less widespread than with QA lesioning (Supp. Info. Fig. 2; compare with Fig. 4I,M). Together with the Tg(*gfap:GFP*) and Tg(*1016tuba1a:GFP*) reporter lines, these data indicate widespread activation of radial glia NPCs after QA lesioning and, to a lesser extent, vehicle-induced injury.

Generation of New Neurons After Injury

To test whether cells that proliferated in response to QA-induced lesioning differentiated into neurons, we performed pulse-chase labeling with EdU at the peak of proliferation 2 dpl and determined whether labeled cells coexpressed the neuronal marker HuC/D at later timepoints. A subset of cells that incorporated EdU at 2 dpl coexpressed the neuronal marker HuC/D as early as 2 days later (4 dpl, Fig. 5A,B). These cells were primarily located in the periventricular area but appeared to be migrating towards the site of injury. By 7 dpl, some EdU-labeled cells remained in the expanded periventricular zone while others appeared in the parenchyma near the injury site, many of which coexpressed HuC/D (Fig. 5C). At 14 dpl, many colabeled cells were seen extending from the periventricular zone with substantial numbers near the injury location (Fig. 5D). By 21 dpl, EdU/HuC/D colabeled cells that had migrated into the parenchyma settled near the damaged area while others took up positions closer to the periventricular zone (Fig. 5E,F). These results suggest that new neurons generated during peak proliferation after injury survive and contribute to repair of QA-induced telencephalic damage.

We next used conditional NPC-specific GFP expression in transgenic zebrafish to map the lineages of progeny derived from VZ neural stem cells of adult zebrafish following injury. VZ radial glial-like cells in the uninjured adult zebrafish brain have been identified as neural stem cells (Rothenaigner et al., 2011). These cells are a heterogeneous population, many of which express radial glial markers such as GFAP, S100β, and vimentin (Ganz et al., 2010). In addition, expression of the Notch target gene *her4* overlaps with radial glial markers in these cells (Kroehne et al., 2011). We used a double transgenic fish line consisting of the *her4* promoter driving expression of a tamoxifen-inducible Cre recombinase (Tg(*her4:CreER^{T2}*)) bred to a pan-neuronal reporter expressing GFP upon Cre-mediated recombination (Tg(*β-actin2:loxp-mCherry-loxp-GFP*), referred to as Tg(*β-actin2:LCLG*)) (Ramachandran et al., 2010). In the uninjured adult zebrafish brain, we found GFP expression in scattered VZ progenitors 4 weeks following intraperitoneal administration of tamoxifen (Fig. 6A). Most of these cells remained in the VZ and did not express the mature neuronal marker HuC/D, although a few settled in the periventricular area with an occasional cell observed in the parenchyma that was HuC/D$^+$ (Fig. 6A inset). These results illustrate a low level of constitutive GFP expression in scattered neural stem cells under noninjury conditions, some of which remain in the VZ, while others produce a limited number of new neurons that migrate out to the periventricular region or into the parenchyma.

The use of intraperitoneal tamoxifen injections likely underestimates the *her4*-expressing NPC population due to low recombination efficiency. Therefore, we subsequently induced recombination at the time of QA lesioning by injecting tamoxifen directly into the brain along with QA. At 1 day after injection, GFP expression was detected in the VZ near the lesion site with a modest number of GFP$^+$ processes extending into the parenchyma (Fig. 6B). GFP expression was more widespread at 3 dpl in VZ cell bodies with GFP$^+$ processes directed toward the lesion site from both medial and lateral VZs (Fig. 6C,D). Within 7 days after injury, the numbers of GFP$^+$ cells increased further in periventricular regions adjacent to damaged sites, and many GFP$^+$ somata were located near the lesioned parenchyma (Fig. 6E). Vehicle lesions with tamoxifen produced similar results although somewhat less extensive GFP expression (Supp. Info. Fig. 3A–C). These findings suggest that NPCs in the VZ are activated by injury to give rise to progeny that migrate toward damaged regions, perhaps along processes of radial glia-like cells that extend from the VZ to the damaged area.

To confirm that *her4*-driven GFP$^+$ cells proliferated in response to QA lesioning, we performed pulse-chase labeling with EdU as a marker of mitotic cells. EdU was injected 2 days after lesioning, and 1 day later many EdU$^+$ cells coexpressed GFP and appeared to extend toward the lesion site (Fig 6F–G). By day 5 after EdU labeling (7 days after injury), large numbers of GFP/EdU colabeled cells appeared near the injured region (Fig 6H,I), suggesting migration into the parenchyma. Many GFP/EdU double positive cells were also present throughout the VZ and periventricular regions near the area of telencephalic damage. GFP$^+$ cells persisted 28 and 56 dpl. At these later timepoints, GFP$^+$ soma were seen in clusters near the injury site as well as in ventricular and periventricular areas (Fig. 6J). Many of these cells coexpressed the neuronal marker HuC/D, identifying them as neurons generated in response to injury (Fig 6J′,K). Similar results were obtained following vehicle lesions (Supp. Info. Fig. 3E–H). In addition, in contrast to the thin, unelaborated processes evident on GFP$^+$ cells emanating from the VZ early after QA injection (Fig. 6C–E), GFP$^+$ neurons identified at later post-injury timepoints showed mature neuronal morphologies with highly elaborated and branched processes (Fig. 6L). Together,

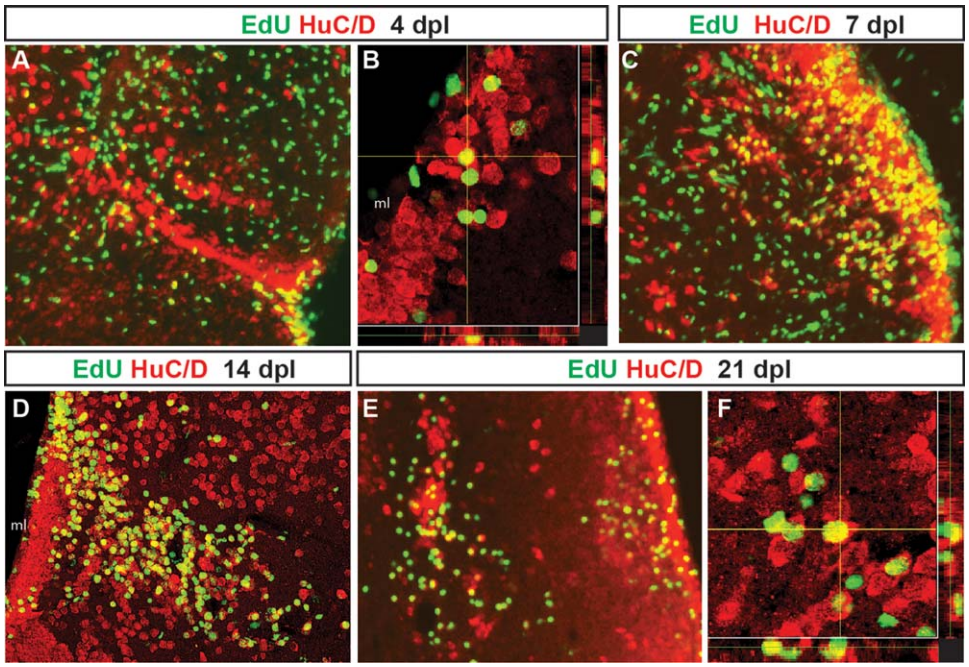

FIGURE 5: Adult-generated cells differentiate into neurons that progressively migrate to the site of injury. Proliferating cells that incorporated EdU at 2 days post-lesion were double labeled for EdU (green) and the neuronal marker HuC/D (red) after different chase periods. A yellow asterisk denotes the injury site in each panel. At 4 days after QA injection, EdU$^+$ cells that express the neuronal marker HuC/D appeared to leave the VZ and extend toward the site of injury (A, orthogonal projection in B). By 7 dpl (C), EdU/HuC/D colabeled cells were found at a distance from the VZ. By 14 (D) and 21 dpl (E, orthogonal projection in F), two distinct populations of newborn neurons were present. Many double-labeled cells settled along the periventricular region where neuronal cell bodies are normally located. Other EdU/HuC/D double-labeled cells were located near the lesion site. Scale bars = 100 μm.

the temporal and spatial patterns of GFP expression, the change in GFP$^+$ cell morphology over time, and incorporation of EdU by many GFP$^+$ cells all indicate that *her4*-driven recombination is restricted to neural progenitors and is not induced in mature neurons after injury.

To repair damaged neural circuitry, it is important that new neurons reestablish not only the correct neuronal phenotypes and local connections, but also that they successfully reestablish connections with long-range targets. We used the intracerebral tamoxifen injection protocol described above to label her4-expressing radial glial stem cells at the time of injury and examine whether the neurons they generate after QA injection establish long-range connections as part of the neural regenerative response. Between 3 and 7 days after QA lesioning, increasing and extensive GFP labeling appeared in the injured dorsal telencephalon near the damaged region and to a lesser extent in ventral regions further from the injury (Fig. 7A–D). At the level of the anterior commissure located ventrally, GFP$^+$ soma and processes were present but largely constrained to the ipsilesional hemisphere at 7 days after injury (Fig. 7D), with limited GFP expression in the uninjured contralesional hemisphere (Fig. 7B). Remarkably, by 14 and 28 days following QA lesioning, GFP$^+$ processes showed aggregated fascicles in the injured hemisphere and extended fiber bundles across the anterior commissure to the contralateral side (Fig. 7E–F″). The ends of the bundles appeared to terminate in more dorsal portions of the contralateral hemisphere (arrows in Fig. 7E,F). We next performed double-label immunofluorescence for the synaptic vesicle marker SV2 and GFP to examine whether GFP$^+$ fibers made synaptic contacts in the contralateral telencephalic hemisphere. At 28 dpl, we observed areas of GFP and SV2 coexpression (Fig 7G,G′), suggesting that GFP$^+$ processes arising from the injured hemisphere make synapses in the contralateral hemisphere. These results indicate that repair occurs not only in the lesioned telencephalic hemisphere, but also importantly that long-range connections are reestablished following injury.

Effective repair of the injured brain also requires that multiple specific neuronal subtypes be generated by the NPCs that proliferate following injury. At 28 days post QA injection, GFP$^+$ cells that incorporated EdU given at the peak of proliferation 26 days earlier (2 dpl) were located near the lesion site, indicating that these cells were newly generated after brain injury (Fig. 8A,A′). GFP-labeled cells present in regenerating regions 28 days after injury also coexpressed the neuronal marker HuC/D (Fig. 8B,B′; see also Fig. 6J,K). We next examined whether specific subtypes of neurons were generated by the NPCs activated in response to injury. Colabeling for GFP and the inhibitory neuronal marker GABA revealed that some newly generated neurons differentiated

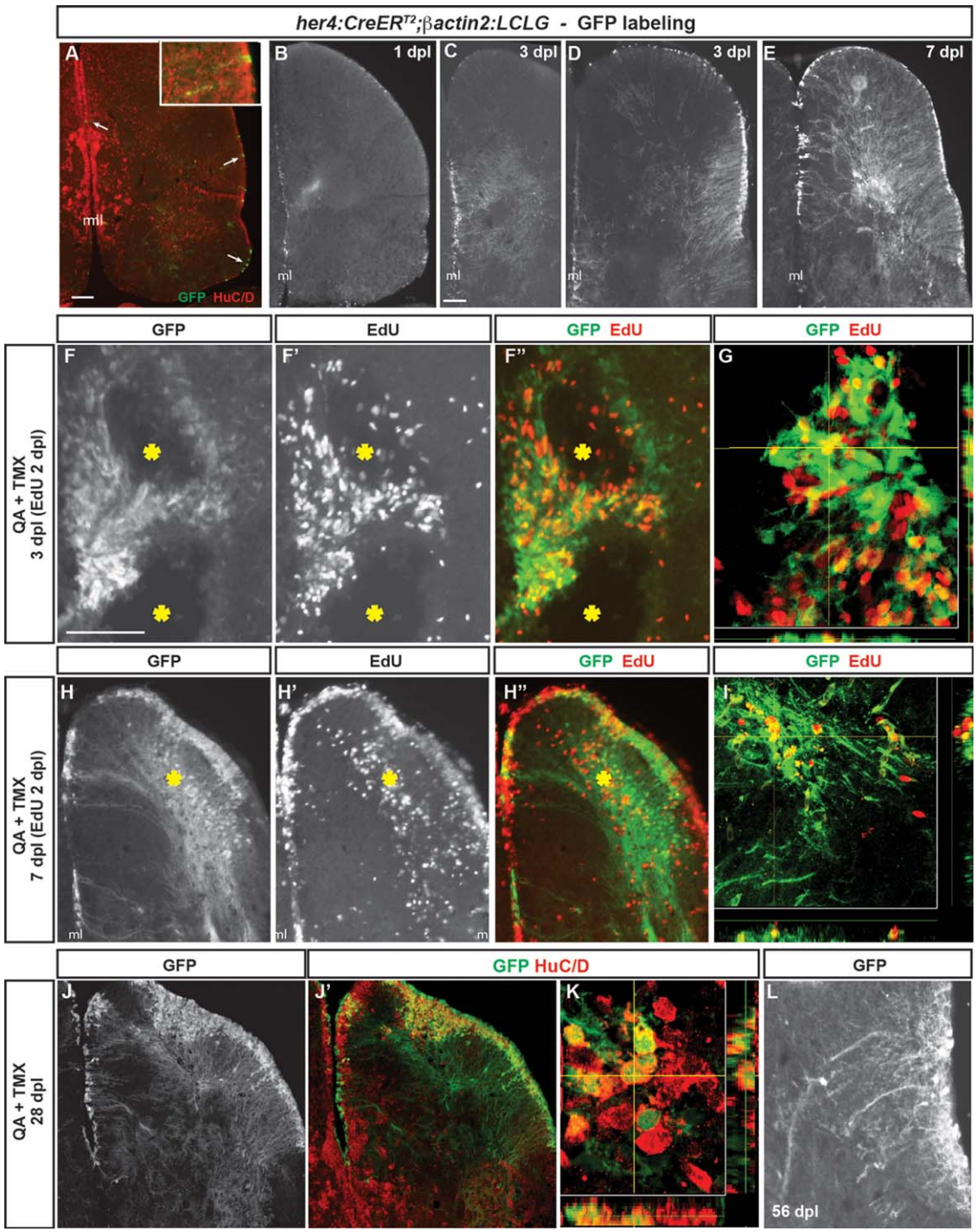

FIGURE 6: Radial glia-specific lineage mapping shows NPC activation, increased neurogenesis and migration to injury after QA-induced telencephalic lesioning. (**A–A″**) A double transgenic zebrafish Tg(*her4:CreER^{T2};β-actin2:LCLG*) received tamoxifen intraperitoneally for 4 days and was examined 4 weeks later. Scattered GFP$^+$ cells (green in A″) appeared in the VZ (arrows) which generated a very small number of GFP$^+$ neurons that extended a short distance from the ventricular surface and coexpressed the neuronal marker HuC/D (red; inset in A″). (**B**) A modest amount of GFP expression was observed in the VZ at 1 dpl after intratelencephalic injection of QA and tamoxifen. (**C,D**) By 3 days after injury, the GFP$^+$ progenitor population expanded in both the medial (C) and lateral (D) periventricular regions. (**E**) By 7 dpl, many GFP$^+$ cell bodies were observed in the VZ, periventricular regions and parenchyma of the QA-lesioned hemisphere, indicating migration to injury, and an extensive network of GFP$^+$ processes extended from the VZ to the lesion site. (**F–F″**) Pulse-chase labeling with EdU (red in F″) administered 2 dpl revealed that, as early as 1 day later, newborn cells derived from GFP$^+$ radial glia extend toward the lesion site (yellow asterisks). (**G**) Orthogonal projection shows a cell colabeled with GFP and EdU that has migrated from the VZ. (**H,I**) Many GFP$^+$ cell bodies that incorporated EdU at 2 dpl appeared in the parenchyma by 7 dpl while others remained in the ventricular/periventricular regions. Large numbers of GFP$^+$ processes also extend from the ventricular region to the injury (yellow asterisk). (**J,K**) Many GFP$^+$ cells (green) in both the parenchyma and periventricular regions remained at 28 dpl and coexpressed the neuronal marker HuC/D (red). (**L**) In contrast to their appearance as long, unelaborated processes at 3 dpl (see C,D), by 56 days after QA injection, GFP$^+$ cells exhibit processes with highly branched, mature morphology. Scale bar = 100 μm. Scale bar in A applies to B. Scale bar in C applies to D, E, H, J. Scale bar in F applies to L. ml = midline.

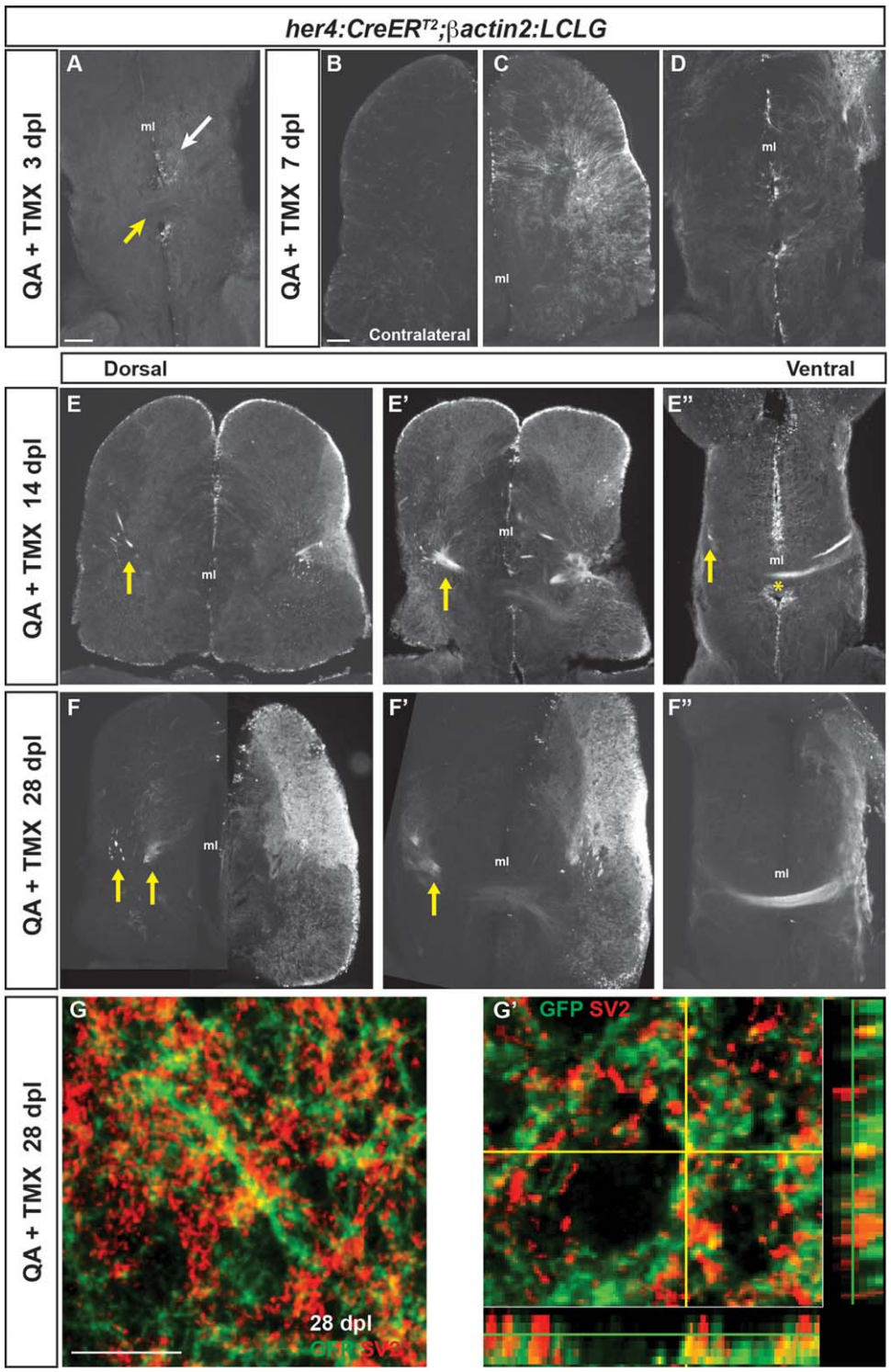

FIGURE 7: Neurons generated after QA-induced brain injury progressively extend processes to reestablish neuronal connections. (**A**) In the ventral telencephalon of Tg(*her4:creER^{T2};β-actin2:LCLG*) fish at 3 dpl, labeled progenitors began to extend GFP$^+$ processes into the ipsilesional parenchyma (white arrow), but GFP expression was absent from the anterior commissure (yellow arrow) and contralateral hemisphere. (**B–D**) At 7 days after QA injection, minimal GFP expression was seen in the contralesional telencephalic hemisphere (B). In contrast, the ipsilesional hemisphere exhibited many GFP$^+$ cells in the VZ and periventricular area that extended processes toward the injury site (C). At the level of the anterior commissure, GFP$^+$ cells and processes were apparent but restricted to the ipsilesional hemisphere at 7 dpl (D). (**E–E″**) Fasciculated bundles of GFP$^+$ processes appeared by 14 dpl in the ipsilesional hemisphere and were also seen contralaterally (arrows) at dorsal levels (E, E′). More ventrally, GFP+ fibers appeared in the contralesional hemisphere (arrow in E″) and a GFP$^+$ fiber bundle crossed at the level of the anterior commissure (E″, asterisk). (**F–F″**) The GFP$^+$ bundles persisted at 28 dpl. At more dorsal levels, GFP$^+$ fascicles were seen in the parenchyma of the contralesional hemisphere (F,F′), and at ventral levels an extensive fiber bundle crossed the anterior commissure (F″). (G–G′) Colabeling for GFP (green) and the synaptic marker SV2 (red) in the contralesional telencephalon at 28 dpl revealed the appearance of synaptic contacts made by GFP$^+$ axons onto putative targets. G′ shows an orthogonal projection of GFP$^+$ synaptic contacts colabeled for SV2 (red). Scale bars = 100 μm. Scale bar in A applies to D, F′, F″; in B to C, E, F. ml = midline.

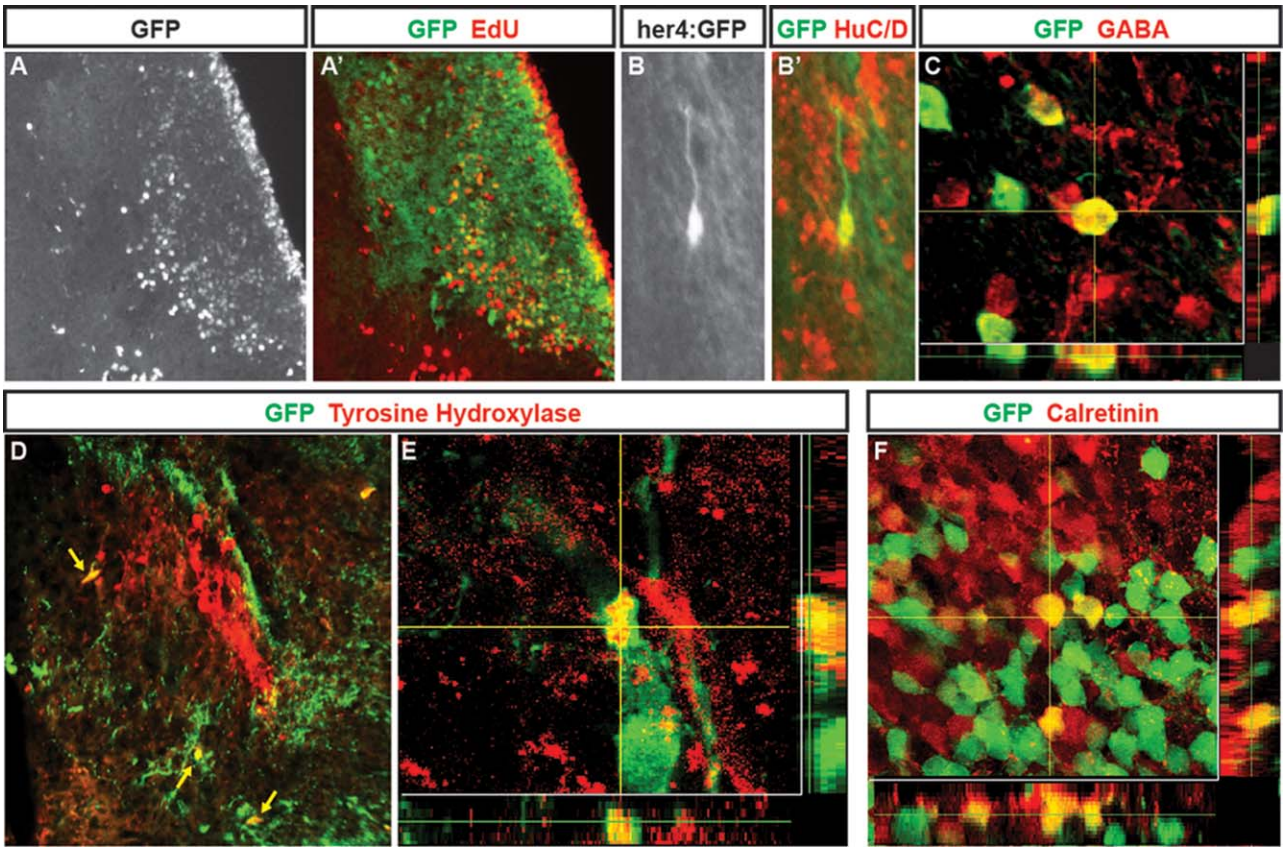

FIGURE 8: Neurons generated following QA-induced lesions of adult zebrafish telencephalon adopt multiple phenotypes. (A, A′) In Tg(*her4:creER^{T2};β-actin2:LCLG*) (her4:GFP) fish at 28 days post-lesioning, cells birthdated with EdU (A; red in A′) at 2 days after QA and tamoxifen injection have settled in the periventricular region and parenchyma of the damaged hemisphere where many coexpress GFP (green in A′). (B–B′) Higher magnification view of a GFP/HuC/D double-labeled cell with neuronal morphology in the parenchyma. (C) Neurons labeled for the inhibitory neuronal marker GABA include cells that coexpress GFP that comingle closely with other GABA-expressing cells. (D,E) Neurons double-labeled (yellow arrows) for GFP (green) and tyrosine hydroxylase (TH) comingle among the distinctive TH positive cluster of cells (red) in the ipsilesional hemisphere. (F) Within a calretinin-expressing group of neurons, some cells coexpressed calretinin (red) and GFP (green) whereas neighboring cells showed immunoreactivity for one of the two markers. Scale bar A, B, D = 100 μm. Scale bar C, E, F = 50 μm.

into GABAergic interneurons in the repaired telencephalon (Fig. 8C). Tyrosine hydroxylase marks a distinctive subset of dopaminergic neurons in the medial telencephalon (Rink and Wullimann, 2001, 2002). We observed cells coexpressing GFP and TH near large groups of TH-immunoreactive neurons at 28 days post injury (Fig. 8D,E). Calretinin is expressed by neurons within the rostral migratory stream and olfactory bulb, as well as specific nuclei in the telencephalon (Castro et al., 2006). We found neurons coexpressing GFP and calretinin in the telencephalic parenchyma at 28 days post injury (Fig. 8F). These findings indicate that *her4*-lineage mapped, GFP$^+$ NPCs activated in response to QA-induced injury generate a diversity of neuronal subtypes with the potential to replace various neurons lost to brain injury.

Discussion

Recent studies have shown that adult zebrafish possess the ability to increase adult NPC proliferation following stab lesions to the telencephalon (Ayari et al., 2010; Diotel et al., 2013; Kishimoto et al., 2012; Kizil et al., 2012a, 2012b; Kroehne et al., 2011; Kyritsis et al., 2012). The activated NPCs give rise to new neurons that appear to participate in the repair of brain injury. In the present study we extend these findings using a novel injury model, QA-induced excitotoxic lesioning. Intracerebral QA injection is a well-established experimental model in rodents for the study of neuronal loss due to acute brain insults or neurodegenerative diseases (Gordon et al., 2007; Guillemin, 2012; Miranda et al., 1999; Schwarcz and Köhler, 1983; Tattersfield et al., 2004). We find that the initial response to QA lesioning in fish, as to stab injury alone, is cell death followed by a rapid accumulation of microglia in the injured hemisphere. This injury response is accompanied by a large increase in proliferation of neurogenic radial glia located in the VZs of the injured hemisphere. Injury-induced changes are largely restricted to the damaged hemisphere, although there is some reactivity in the contralateral hemisphere, much more in QA-

than in vehicle-injected fish. Within the injured hemisphere, QA-induced lesioning stimulates an intense microglial reaction, NPC proliferation and damage repair, all to a greater extent than after vehicle injection. We also find that the radial glial NPCs responding to QA-induced injury generate several neuronal subtypes, as well as neurons that give rise to long-distance projections that cross the anterior commissure and reestablish synaptic connections with the contralesional hemisphere.

Why does QA-induced injury exert a more widespread and powerful stimulation of inflammation and regenerative responses than mechanical injury alone? One possibility involves potential direct actions of QA on glutamate receptors. Glutamatergic neurotransmission has been shown to exert effects on adult neurogenesis in mammals (Deisseroth et al., 2004), particularly through the activation of *N*-methyl-D-aspartate (NMDA) receptors upon which QA acts (Luk et al., 2003; Orlando et al., 2001), although NMDA receptor activation tends to acutely decrease neurogenesis in the adult rodent hippocampus (Cameron et al., 1995). Another potential explanation is through a QA-induced increase in neuronal excitability that occurs as part of the excitotoxicity it produces. Such neuronal activation is suggested by the acute circling behavior observed in fish after QA injection that was not seen with vehicle injection (Supp. Info. Movie). This type of behavior in rodents indicates an asymmetry in striatal activity (Hebb and Robertson, 1999; Miranda et al., 1999; Schwarcz et al., 1979; Ungerstedt, 1971). This effect is likely due to ipsilesional excitation by QA in the fish, given that both QA and vehicle injections induce injury and should not differ if the behavior was caused by acute loss of function from damage. Increased excitation in the form of seizures is know to stimulate both inflammation and neurogenesis (Bonde et al., 2006; Bovolenta et al., 2010), although we did not observe behavioral seizures after QA injection. However, even more modest increases in neuronal activity induce progenitor cells to increase neuronal production (Bengzon et al., 1997). Evidence suggests that QA also directly stimulates microglial proliferation *in vitro* (Di Serio et al., 2005; Figueiredo et al., 2008) and this effect may contribute to the increased microglial accumulation after QA administration *in vivo*. The increased microglial reaction in turn may contribute to the enhanced and more complete regeneration after QA lesioning than was seen with vehicle injection alone.

Radial glia persist in the adult zebrafish brain, lining the medial and everted lateral VZs, and they constitutively generate new neurons throughout life (Rothenaigner et al., 2011). Most of these cells express the radial glial markers GFAP, vimentin, and S100β, although they are a heterogeneous population some of which are negative for glial markers (Ganz et al., 2010). A large subset of these cells expresses the Notch target gene *her4* as shown by our data and by others (Chapouton et al., 2011; Kroehne et al., 2011). Activation of Notch signaling is required for injury-induced proliferation of forebrain progenitors in zebrafish and rodents (Givogri et al., 2006; Kishimoto et al., 2012; Wang et al., 2009). We show that new neurons are derived from her4-expressing progenitors following QA-induced injury, but the degree of radial glial activation and subsequent neurogenesis determined by transgenic lineage mapping is greater in our QA lesion model than that reported in previous studies. Although this in part may reflect our use of QA rather than simply mechanical injury, a more important factor is probably the route of tamoxifen administration we use to induce recombination. Several factors support the specificity of intracerebral tamoxifen delivery at the time of injury, which is much more effective than intraperitoneal tamoxifen injection for inducing CreER-mediated telencephalic recombination in fish (Fig. 6). First, a time course of lineage mapping after tamoxifen injection indicates that VZ cells are initially activated and over time give rise to progeny that migrate into the parenchyma and differentiate into neurons. Second, mitotic labeling shows that many of the GFP^+ cells were in S-phase at the time of EdU administration, confirming their proliferative NPC behavior. Finally, the GFP^+ neurons initially display immature morphologies that evolve to more mature phenotypes over time after tamoxifen injection. With this lineage mapping approach we confirm the radial glial source of the neurons generated after injury and reveal a profound neurogenic response that likely accounts for repair of the injured telencephalon in response to QA lesioning.

Remarkably, our *her4* lineage mapping shows that neurons generated after QA-induced injury send long-distance projections across the anterior commissure to synapse in the uninjured hemisphere. These telencephalic commissural fibers in the fish are not well described. A developmental study has characterized axon guidance factors required by distinct populations of neurons that extend commissural fibers from the telencephalon (Zhang et al., 2012). In addition, commissurally projecting neurons from the rostro-dorso-lateral telencephalon of another species of teleost fish have been identified (Corrêa et al., 1998). When labeled by injection of axonal tracers in adult fish, these latter cells are found to send projections across the commissure that terminate in the dorsal telencephalon of the contralateral hemisphere. These fiber terminations look remarkably similar to the pattern of GFP labeling we see in the uninjured hemisphere, which arise from adult-generated cells in the damaged telencephalic hemisphere. Further investigation is necessary to determine the specific neuronal subtypes that give rise to the anterior commissural projections, as well as the potential functional integrity of the regenerated neuronal circuits. However, our results suggest that the fiber bundles coalesce and organize over time

(Fig. 7), which may reflect stable integration of the adult-generated neuronal circuitry.

Although it is clear that the injured adult zebrafish telencephalon has a remarkable capacity to regenerate by upregulation of proliferation, generation of new neurons, and differentiation into multiple neuronal subtypes, many questions about the regeneration process remain to be answered. The molecular and cellular factors driving regeneration are poorly understood. One of the earliest responses to brain lesion is a robust inflammatory reaction. Microglia infiltrate, proliferate, and become activated in large numbers. Chronic inflammation and glial scarring have long been considered major hindrances to repair in the mammalian CNS (Fitch and Silver, 2008; Hoehn et al., 2005; Rasmussen et al., 2011; Sofroniew, 2009). However, both positive and negative effects on neurogenesis and repair have been reported (Ekdahl et al., 2009). Neurogenesis and survival of new neurons is increased following apoptotic neuronal ablation that does not result in an inflammatory response (Chen et al., 2004; Magavi et al., 2000). In contrast, microglial accumulation following stroke can promote neurogenesis and subsequent neuronal survival (Thored et al., 2009). A recent study in zebrafish suggests that the inflammatory response is required to initiate neurogenic proliferation in the adult VZ through pathways that are distinct from those regulating constitutive neurogenesis (Kyritsis et al., 2012). By contrast, the injured adult zebrafish brain does not exhibit widespread persistent inflammation or glial scarring (Baumgart et al., 2011). This lack of later-stage inflammation may lead to successful neuronal repair in the zebrafish brain, although the mechanism by which damping of the inflammatory response occurs is not known. Differences in signaling by microglia that react to injury in zebrafish and receptor expression on responding radial glia have yet to be investigated and will provide an informative comparison with species, location, and injury-type differences described in mammalian models (Christie and Turnley, 2013).

The signals that attract radial glial scaffolding processes to the lesion site or direct the migration of newly generated neurons to damaged regions and outgrowth of their processes to targets in the contralateral hemisphere are as yet unknown. QA-induced or focal ischemic lesions in mouse result in the upregulation of chemokines that serve as attractants for the migration of SVZ-derived NPCs to sites of brain injury (Gordon et al., 2009; Ohab et al., 2006). These chemokines are expressed by microglia, macrophages and astrocytes at the injury site and their appearance is accompanied by upregulation of receptor expression in SVZ-derived cells. There have been no reports describing expression in adult zebrafish of the same chemokines involved in directing the migration of neuroblasts in rodent stroke models, such as stromal-derived factor 1 (Ohab et al., 2006), with the exception of the chemokine Prokineticin 2, whose expression is upregulated following zebrafish brain injury and may guide the migration of new neurons to the injury site (Ayari et al., 2010). One study, however, found that the chemokine receptor CXCR5 was upregulated at early timepoints in radial glial progenitors that respond to injury, although the identity of its ligand is unknown (Kizil et al., 2012a).

Results from the present study provide a novel injury model for exploring neuronal regeneration in an adult vertebrate. QA lesioning is a well-established model for neurodegeneration and neuronal damage in mammalian systems. We have shown that it can also be used as a powerful brain injury model in adult zebrafish, one which may more closely mimic the mechanisms of secondary damage that occur following brain injury or disease in mammalian systems than does stab injury alone. Future examination of differences in molecular signals elicited by QA versus vehicle lesioning may shed light on unique repair mechanisms that allow for complete brain tissue restoration. We find a difference in the acute behavioral response to QA when compared with vehicle injection and it would also be interesting to explore potential longer-term behavioral correlates of the injury and subsequent recovery. In addition, further comparative studies using zebrafish and mammalian systems should prove useful in identifying common mechanisms of neuronal regeneration as well as elucidating mechanistic and environmental differences between zebrafish and mammalian brains that are permissive for regeneration in the former but restrict regeneration in the latter. Finally, QA-induced brain lesioning in fish offers a potent model system to test potential therapies to enhance recovery after brain insults or neurodegeneration that may be translated to mammalian brain repair.

Acknowledgment

Grant sponsor: National Institutes of Health; Grant number: NS061293 (to J.M.P.), EY018132 (to D.G.), and NS007222 (to K.S.).

The authors thank Randall Karr for zebrafish care and Bruce Appel, Weibin Chen, David Hyde, and Rajesh Ramachandran for supplying transgenic fish.

References

Adolf B, Chapouton P, Lam CS, Topp S, Tannhauser B, Strähle U, Götz M, Bally-Cuif L. 2006. Conserved and acquired features of adult neurogenesis in the zebrafish telencephalon. Dev Biol 295:278–293.

Arvidsson A, Collin T, Kirik D, Kokaia Z, Lindvall O. 2002. Neuronal replacement from endogenous precursors in the adult brain after stroke. Nat Med 8: 963–970.

Ayari B, El Hachimi KH, Yanicostas C, Landoulsi A, Soussi-Yanicostas N. 2010. Prokineticin 2 expression is associated with neural repair of injured adult zebrafish telencephalon. J Neurotr 27:959–972.

Baumgart EV, Barbosa JS, Bally-Cuif L, Götz M, Ninkovic J. 2011. Stab wound injury of the zebrafish telencephalon: A model for comparative analysis of reactive gliosis. Glia:343–357.

Beal MF, Kowall NW, Ellison DW, Mazurek MF, Swartz KJ, Martin JB. 1986. Replication of the neurochemical characteristics of Huntington's disease by quinolinic acid. Nature 321:168–171.

Becker CG, Becker T. 2007. Growth and pathfinding of regenerating axons in the optic projection of adult fish. J Neurosci Res 85:2793–2799.

Becker CG, Becker T. 2008. Adult zebrafish as a model for successful central nervous system regeneration. Restorat Neurol Neurosci 26:71–80.

Becker T, Becker CG. 2001. Regenerating descending axons preferentially reroute to the gray matter in the presence of a general macrophage/microglial reaction caudal to a spinal transection in adult zebrafish. J Compar Neurol 433:131–147.

Becker T, Wullimann MF, Becker CG, Bernhardt RR, Schachner M. 1997. Axonal regrowth after spinal cord transection in adult zebrafish. The J Compar Neurol 377:577–595.

Bengzon J, Kokaia Z, Elmér E, Nanobashvili A, Kokaia M, Lindvall O. 1997. Apoptosis and proliferation of dentate gyrus neurons after single and intermittent limbic seizures. Proc Natl Acad Sci USA 94:10432–10437.

Benjamins JA, Nedelkoska L, Bealmear B, Lisak RP. 2013. ACTH protects mature oligodendroglia from excitotoxic and inflammation-related damage in vitro. Glia 61:1206–1217.

Bernardos RL, Barthel LK, Meyers JR, Raymond PA. 2007. Late-stage neuronal progenitors in the retina are radial Müller glia that function as retinal stem cells. J Neurosci 27:7028–7040.

Bertrand N, Castro DS, Guillemot F. 2002. Proneural genes and the specification of neural cell types. Nat Rev Neurosci 3:517–530.

Bonde S, Ekdahl CT, Lindvall O. 2006. Long-term neuronal replacement in adult rat hippocampus after status epilepticus despite chronic inflammation. Eur J Neurosci 23:965–974.

Boniface EJ, Lu J, Victoroff T, Zhu M, Chen W. 2009. FlEx-based transgenic reporter lines for visualization of Cre and Flp activity in live zebrafish. Genesis 47:484–491.

Bovolenta R, Zucchini S, Paradiso B, Rodi D, Merigo F, Navarro Mora G, Osculati F, Berto E, Marconi P, Marzola A, Fabene PF, Simonato M. 2010. Hippocampal FGF-2 and BDNF overexpression attenuates epileptogenesis-associated neuroinflammation and reduces spontaneous recurrent seizures. J Neuroinflammation 7:81–86. .

Buffo A, Vosko MR, Ertürk D, Hamann GF, Jucker M, Rowitch D, Götz M. 2005. Expression pattern of the transcription factor Olig2 in response to brain injuries: Implications for neuronal repair. Proc Natl Acad Sci USA 102:18183–18188.

Cameron HA, McEwen BS, Gould E. 1995. Regulation of adult neurogenesis by excitatory input and NMDA receptor activation in the dentate gyrus. J Neurosci 15:4687–4692.

Cammer W. 2001. Oligodendrocyte killing by quinolinic acid in vitro. Brain Res 896:157–160.

Castro A, Becerra M, Manso MJ, Anadón R. 2006. Calretinin immunoreactivity in the brain of the zebrafish, Danio rerio: Distribution and comparison with some neuropeptides and neurotransmitter-synthesizing enzymes. I. Olfactory organ and forebrain. J Comparative Neurol 494:435–459.

Chapouton P, Skupien P, Hesl B, Coolen M, Moore JC, Madelaine R, Kremmer E, Faus-Kessler T, Blader P, Lawson ND, Bally-Cuif L. 2010. Notch activity levels control the balance between quiescence and recruitment of adult neural stem cells. J Neurosci 30:7961–7974.

Chapouton P, Webb KJ, Stigloher C, Alunni A, Adolf B, Hesl B, Topp S, Kremmer E, Bally-Cuif L. 2011. Expression of hairy/enhancer of split genes in neural progenitors and neurogenesis domains of the adult zebrafish brain. J Comparative Neurol 519:1748–1769.

Chen J, Magavi SSP, Macklis JD. 2004. Neurogenesis of corticospinal motor neurons extending spinal projections in adult mice. Proc Natl Acad Sci USA 101:16357–16362.

Christie K, Turnley A. 2013. Regulation of endogenous neural stem/progenitor cells for neural repair—Factors that promote neurogenesis and gliogenesis in the normal and damaged brain. Frontiers Cellular Neurosci 6:70.

Clint SC, Zupanc GKH. 2001. Neuronal regeneration in the cerebellum of adult teleost fish, Apteronotus leptorhynchus: Guidance of migrating young cells by radial glia. Dev Brain Res 130:15–23.

Collin T, Arvidsson A, Kokaia Z, Lindvall O. 2005. Quantitative analysis of the generation of different striatal neuronal subtypes in the adult brain following excitotoxic injury. Exp Neurol 195:71–80.

Corrêa SAL, Grant K, Hoffmann A. 1998. Afferent and efferent connections of the dorsocentral telencephalon in an electrosensory teleost, *Gymnotus carapo*. Brain Behav Evol 52:81–98.

Darlington LG, Mackay GM, Forrest CM, Stoy N, George C, Stone TW. 2007. Altered kynurenine metabolism correlates with infarct volume in stroke. Eur J Neurosci 26:2211–2221.

Deisseroth K, Singla S, Toda H, Monje M, Palmer TD, Malenka RC. 2004. Excitation-neurogenesis coupling in adult neural stem/progenitor cells. Neuron 42:535–552.

Di Serio C, Cozzi A, Angeli I, Doria L, Micucci I, Pellerito S, Mirone P, Masotti G, Moroni F, Tarantini F. 2005. Kynurenic acid inhibits the release of the neurotrophic fibroblast growth factor (FGF)−1 and enhances proliferation of glia cells, in vitro. Cell Mol Neurobiol 25:981–993.

Diotel N, Vaillant C, Gabbero C, Mironov S, Fostier A, Gueguen M-M, Anglade I, Kah O, Pellegrini E. 2013. Effects of estradiol in adult neurogenesis and brain repair in zebrafish. Horm Behav 63:193–207.

Ekdahl CT, Kokaia Z, Lindvall O. 2009. Brain inflammation and adult neurogenesis: The dual role of microglia. Neuroscience 158:1021–1029.

Fausett BV, Goldman D. 2006. A role for α1 tubulin-expressing Müller glia in regeneration of the injured zebrafish retina. J Neurosci 26:6303–6313.

Fausett BV, Gumerson JD, Goldman D. 2008. The proneural basic helix-loop-helix gene Ascl1a is required for retina regeneration. J Neurosci 28:1109–1117.

Ferrante RJ, Kowall NW, Cipolloni PB, Storey E, Beal MF. 1993. Excitotoxin lesions in primates as a model for Huntington's Disease: Histopathologic and neurochemical characterization. Exp Neurol 119:46–71.

Figueiredo C, Pais TF, Gomes JR, Chatterjee S. 2008. Neuron-microglia crosstalk up-regulates neuronal FGF-2 expression which mediates neuroprotection against excitotoxicity via JNK1/2. J Neurochem 107:73–85.

Fitch MT, Silver J. 2008. CNS injury, glial scars, and inflammation: Inhibitory extracellular matrices and regeneration failure. Exp Neurol 209:294–301.

Ganz J, Kaslin J, Freudenreich D, Machate A, Geffarth M, Brand M. 2012. Subdivisions of the adult zebrafish subpallium by molecular marker analysis. J Compar Neurol 520:633–655.

Ganz J, Kaslin J, Hochmann S, Freudenreich D, Brand M. 2010. Heterogeneity and Fgf dependence of adult neural progenitors in the zebrafish telencephalon. Glia 58:1345–1363.

Givogri MI, de Planell M, Galbiati F, Superchi D, Gritti A, Vescovi AL, de Vellis J, Bongarzone ER. 2006. Notch signaling in astrocytes and neuroblasts of the adult subventricular zone in health and after cortical injury. Dev Neurosci 28:81–91.

Gordon RJ, McGregor AL, Connor B. 2009. Chemokines direct neural progenitor cell migration following striatal cell loss. Mol Cell Neurosci 41:219–232.

Gordon RJ, Tattersfield AS, Vazey EM, Kells AP, McGregor AL, Hughes SM, Connor B. 2007. Temporal profile of subventricular zone progenitor cell migration following quinolinic acid–induced striatal cell loss. Neuroscience 146:1704–1718.

Grandel H, Kaslin J, Ganz J, Wenzel I, Brand M. 2006. Neural stem cells and neurogenesis in the adult zebrafish brain: Origin, proliferation dynamics, migration and cell fate. Dev Biol 295:263–277.

Guillemin GJ. 2012. Quinolinic acid, the inescapable neurotoxin. FEBS J 279: 1356–1365.

Hebb MO, Robertson HA. 1999. Synergistic influences of the striatum and the globus pallidus on postural and locomotor control. Neuroscience 90:413–421.

Hoehn BD, Palmer TD, Steinberg GK. 2005. Neurogenesis in rats after focal cerebral ischemia is wnhanced by indomethacin. Stroke 36:2718–2724.

Hui SP, Dutta A, Ghosh S. 2010. Cellular response after crush injury in adult zebrafish spinal cord. Dev Dyn 239:2962–2979.

Jin K, Minami M, Lan JQ, Mao XO, Batteur S, Simon RP, Greenberg DA. 2001. Neurogenesis in dentate subgranular zone and rostral subventricular zone after focal cerebral ischemia in the rat. Proc Natl Acad Sci USA 98: 4710–4715.

Jin K, Sun Y, Xie L, Peel A, Mao XO, Batteur S, Greenberg DA. 2003. Directed migration of neuronal precursors into the ischemic cerebral cortex and striatum. Mol Cell Neurosci 24:171–189.

Karadottir R, Cavelier P, Bergersen LH, Attwell D. 2005. NMDA receptors are expressed in oligodendrocytes and activated in ischaemia. Nature 438:1162–1166.

Kernie SG, Parent JM. 2010. Forebrain neurogenesis after focal ischemic and traumatic brain injury. Neurobiol Dis 37:267–274.

Kim EJ, Ables JL, Dickel LK, Eisch AJ, Johnson JE. 2011. Ascl1 (Mash1) defines cells with long-term neurogenic potential in subgranular and subventricular zones in adult mouse brain. PLoS ONE 6:e18472.

Kishimoto N, Shimizu K, Sawamoto K. 2012. Neuronal regeneration in a zebrafish model of adult brain injury. Dis Models Mech 5:200–209.

Kizil C, Dudczig S, Kyritsis N, Machate A, Blaesche J, Kroehne V, Brand M. 2012a. The chemokine receptor cxcr5 regulates the regenerative neurogenesis response in the adult zebrafish brain. Neural Dev 7:27.

Kizil C, Kyritsis N, Dudczig S, Kroehne V, Freudenreich D, Kaslin J, Brand M. 2012b. Regenerative neurogenesis from neural progenitor cells requires injury-induced expression of Gata3. Dev Cell 23:1230–1237.

Kroehne V, Freudenreich D, Hans S, Kaslin J, Brand M. 2011. Regeneration of the adult zebrafish brain from neurogenic radial glia-type progenitors. Development 138:4831–4841.

Kyritsis N, Kizil C, Zocher S, Kroehne V, Kaslin J, Freudenreich D, Iltzsche A, Brand M. 2012. Acute inflammation initiates the regenerative response in the adult zebrafish brain. Science 338:1353–1356.

Lapin IP. 1978. Stimulant and convulsive effects of kynurenines injected into brain ventricles in mice. J Neural Transm 42:37–43.

Luk KC, Kennedy TE, Sadikot AF. 2003. Glutamate promotes proliferation of striatal neuronal progenitors by an NMDA receptor-mediated mechanism. J Neurosci 23:2239–2250.

Magavi SS, Leavitt BR, Macklis JD. 2000. Induction of neurogenesis in the neocortex of adult mice. Nature 405:951–955.

März M, Chapouton P, Diotel N, Vaillant C, Hesl B, Takamiya M, Lam CS, Kah O, Bally-Cuif L, Strähle U. 2010. Heterogeneity in progenitor cell subtypes in the ventricular zone of the zebrafish adult telencephalon. Glia 58: 870–888.

März M, Schmidt R, Rastegar S, Strähle U. 2011. Regenerative response following stab injury in the adult zebrafish telencephalon. Dev Dyn 240:2221–2231.

Miranda AF, Sutton MA, Beninger RJ, Jhamandas K, Boegman RJ. 1999. Quinolinic acid lesion of the nigrostriatal pathway: Effect on turning behaviour and protection by elevation of endogenous kynurenic acid in rattus norvegicus. Neurosci Lett 262:81–84.

Ohab JJ, Fleming S, Blesch A, Carmichael ST. 2006. A neurovascular niche for neurogenesis after stroke. J Neurosci 26:13007–13016.

Orlando LR, Alsdorf SA, Penney Jr JB, Young AB. 2001. The role of group I and group II metabotropic glutamate receptors in modulation of striatal NMDA and quinolinic acid toxicity. Exp Neurol 167:196–204.

Parent JM, Vexler ZS, Gong C, Derugin N, Ferriero DM. 2002. Rat forebrain neurogenesis and striatal neuron replacement after focal stroke. Ann Neurol 52:802–813.

Pellegrini E, Mouriec K, Anglade I, Menuet A, Le Page Y, Gueguen M-M, Marmignon M-H, Brion F, Pakdel F, Kah O. 2007. Identification of aromatase-positive radial glial cells as progenitor cells in the ventricular layer of the forebrain in zebrafish. J Comparative Neurol 501:150–167.

Plane JM, Liu R, Wang T-W, Silverstein FS, Parent JM. 2004. Neonatal hypoxic–ischemic injury increases forebrain subventricular zone neurogenesis in the mouse. Neurobiol Dis 16:585–595.

Ramachandran R, Reifler A, Parent JM, Goldman D. 2010. Conditional gene expression and lineage tracing of tuba1a expressing cells during zebrafish development and retina regeneration. J Comparative Neurol 518:4196–4212.

Ramachandran R, Zhao X-F, Goldman D. 2011. Ascl1a/Dkk/beta-catenin signaling pathway is necessary and glycogen synthase kinase-3beta inhibition is sufficient for zebrafish retina regeneration. Proc Natl Acad Sci USA 108: 15858–15863.

Rasmussen S, Imitola J, Ayuso-Sacido A, Wang Y, Starossom SC, Kivisäkk P, Zhu B, Meyer M, Bronson RT, Garcia-Verdugo JM, Khoury SJ. 2011. Reversible neural stem cell niche dysfunction in a model of multiple sclerosis. Ann Neurol 69:878–891.

Reimer MM, Sörensen I, Kuscha V, Frank RE, Liu C, Becker CG, Becker T. 2008. Motor neuron regeneration in adult zebrafish. J Neurosci 28:8510–8516.

Rink E, Wullimann MF. 2001. The teleostean (zebrafish) dopaminergic system ascending to the subpallium (stratum) is located in the basal diencephalon (posterior tuberculum). Brain Res 889:316–330.

Rink E, Wullimann MF. 2002. Connections of the ventral telencephalon and tyrosine hydroxylase distribution in the zebrafish brain (Danio rerio) lead to identification of an ascending dopaminergic system in a teleost. Brain Res Bull 57:385–387.

Robel S, Berninger B, Götz M. 2011. The stem cell potential of glia: Lessons from reactive gliosis. Nat Revis Neurosci 12:88–104.

Rothenaigner I, Krecsmarik M, Hayes JA, Bahn B, Lepier A, Fortin G, G√∂tz M, Jagasia R, Bally-Cuif L. 2011. Clonal analysis by distinct viral vectors identifies bona fide neural stem cells in the adult zebrafish telencephalon and characterizes their division properties and fate. Development 138:1459–1469.

Schwarcz R, Bruno JP, Muchowski PJ, Wu H-Q. 2012. Kynurenines in the mammalian brain: When physiology meets pathology. Nat Rev Neurosci 13: 465–477.

Schwarcz R, Fuxe K, Agnati LF, Hökfelt T, Coyle JT. 1979. Rotational behaviour in rats with unilateral striatal kainic acid lesions: A behavioural model for studies on intact dopamine receptors. Brain Res 170:485–495.

Schwarcz R, Köhler C. 1983. Differential vulnerability of central neurons of the rat to quinolinic acid. Neurosci Lett 38:85–90.

Shin J, Park H, Topczewska J, Mawdsley D, Appel B. 2003. Neural cell fate analysis in zebrafish using olig2 BAC transgenics. Meth Cell Sci 25:7–14.

Sirbulescu RF, Zupanc GKH. 2011. Spinal cord repair in regeneration-competent vertebrates: Adult teleost fish as a model system. Brain Res Rev 67:73–93.

Sofroniew MV. 2005. Reactive astrocytes in neural repair and protection. Neuroscientist 11:400–407.

Sofroniew MV. 2009. Molecular dissection of reactive astrogliosis and glial scar formation. Trends Neurosci 32:638–647.

Stone T, Forrest C, Stoy N, Darlington L. 2012. Involvement of kynurenines in Huntington's disease and stroke-induced brain damage. J Neural Transm 119:261–274.

Tattersfield AS, Croon RJ, Liu YW, Kells AP, Faull RLM, Connor B. 2004. Neurogenesis in the striatum of the quinolinic acid lesion model of Huntington's disease. Neuroscience 127:319–332.

Thored P, Arvidsson A, Cacci E, Ahlenius H, Kallur T, Darsalia V, Ekdahl CT, Kokaia Z, Lindvall O. 2006. Persistent production of neurons from adult brain stem cells during recovery after stroke. Stem Cells 24:739–747.

Thored P, Heldmann U, Gomes-Leal W, Gisler R, Darsalia V, Taneera J, Nygren JM, Jacobsen S-EW, Ekdahl CT, Kokaia Z, Lindvall O. 2009. Long-term accumulation of microglia with proneurogenic phenotype concomitant with persistent neurogenesis in adult subventricular zone after stroke. Glia 57: 835–849.

Ungerstedt U. 1971. Striatal dopamine release after amphetamine or nerve degeneration revealed by rotational behaviour. Acta physiol Scand Suppl 367:49–68.

Veldman MB, Bemben MA, Goldman D. 2010. Tuba1a gene expression is regulated by KLF6/7 and is necessary for CNS development and regeneration in zebrafish. Mol Cell Neurosci 43:370–383.

Veldman MB, Bemben MA, Thompson RC, Goldman D. 2007. Gene expression analysis of zebrafish retinal ganglion cells during optic nerve regeneration identifies KLF6a and KLF7a as important regulators of axon regeneration. Dev Biol 312:596–612.

Wan J, Ramachandran R, Goldman D. 2012. HB-EGF Is necessary and sufficient for Müller glia dedifferentiation and retina regeneration. Dev Cell 22: 334–347.

Wang L, Chopp M, Zhang RL, Zhang L, LeTourneau Y, Feng YF, Jiang A, Morris DC, Zhang ZG. 2009. The Notch pathway mediates expansion of a progenitor pool and neuronal differentiation in adult neural progenitor cells after stroke. Neuroscience 158:1356–1363.

Yamashita T, Ninomiya M, Hernandez Acosta P, Garcia-Verdugo JM, Sunabori T, Sakaguchi M, Adachi K, Kojima T, Hirota Y, Kawase T, Araki N, Abe K, Okano H, Sawamoto K. 2006. Subventricular zone-derived neuroblasts migrate and differentiate into mature neurons in the post-stroke adult striatum. J Neurosci 26:6627–6636.

Yiu G, He Z. 2006. Glial inhibition of CNS axon regeneration. Nat Rev Neurosci 7:617–627.

Yurco P, Cameron DA. 2005. Responses of Müller glia to retinal injury in adult zebrafish. Vision Res 45:991–1002.

Zhang C, Gao J, Zhang H, Sun L, Peng G. 2012. Robo2–Slit and Dcc–Netrin1 coordinate neuron axonal pathfinding within the embryonic axon tracts. J Neurosci 32:12589–12602.

Zhang RL, Chopp M, Roberts C, Jia L, Wei M, Lu M, Wang X, Pourabdollah S, Zhang ZG. 2011. Ascl1 lineage cells contribute to ischemia-induced neurogenesis and oligodendrogenesis. J Cereb Blood Flow Metab 31:614–625.

Zhang RL, Zhang ZG, Zhang L, Chopp M. 2001. Proliferation and differentiation of progenitor cells in the cortex and the subventricular zone in the adult rat after focal cerebral ischemia. Neuroscience 105:33–41.

Zupanc GKH. 2008. Adult neurogenesis and neuronal regeneration in the brain of teleost fish. J Physiol 102:357–373.

Zupanc GKH, Hinsch K, Gage FH. 2005. Proliferation, migration, neuronal differentiation, and long-term survival of new cells in the adult zebrafish brain. J Comparative Neurol 488:290–319.

Zupanc GKH, Ott R. 1999. Cell proliferation after lesions in the cerebellum of adult teleost fish: Time course, origin, and type of new cells produced. Exp Neurol 160:78–87.

Zupanc MM, Zupanc GKH. 2006. Upregulation of calbindin-D28k expression during regeneration in the adult fish cerebellum. Brain Res 1095:26–34.

Zwilling D, Huang S-Y, Sathyasaikumar KV, Notarangelo FM, Guidetti P, Wu H-Q, Lee J, Truong J, Andrews-Zwilling Y, Hsieh EW, Louie JY, Wu T, Scearce-Levie K, Patrick C, Adame A, Giorgini F, Moussaoui S, Laue G, Rassoulpour A, Flik G, Huang Y, Muchowski JM, Masliah E, Schwarcz R, Muchowski PJ. 2011. Kynurenine 3-monooxygenase inhibition in blood ameliorates neurodegeneration. Cell 145:863–874.